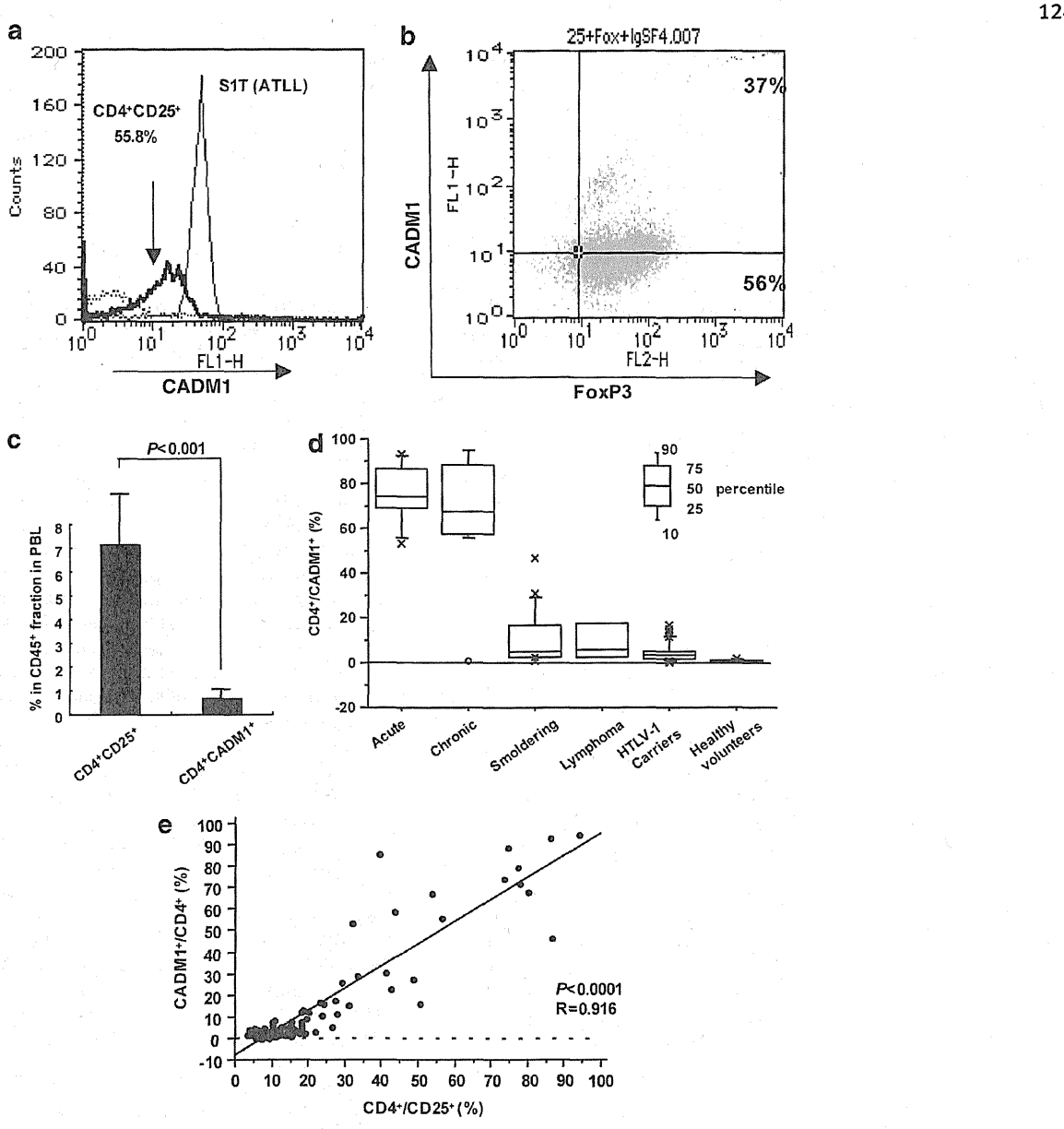

Figure 2. Flow cytometric analysis of CADM1 in T-reg lymphocytes, ATLL cells and HTLV-1-infected T cells. (**a**) Flow cytometric analysis of CADM1 expression in the $CD4^+CD25^+$ fraction from peripheral T lymphocytes. Each sample was stained with an Alexa 488-labeled anti-CADM1 antibody. The S1T-ATLL cell line with high CADM1 expression was used as a positive control. (**b**) The $CD4^+CD25^+$ fraction from peripheral lymphocytes was stained by the Alexa 488-labeled anti-CADM1 and PE-labeled anti-FoxP3 antibodies. (**c**) Comparison of percentages between the $CD4^+CD25^+$ and $CD4^+CADM1^+$ cell fractions in the $CD45^+$ fraction of peripheral blood lymphocytes. (**d**) Box plots are shown for the percentages of the $CD4^+CADM1^+$ cell fractions in $CD45^+$ peripheral blood lymphocytes from patients with various types of ATLL, HTLV-1 carriers and healthy volunteers. The data from a CD4-negative ATLL case are indicated by a white circle. (**e**) Comparison between $CD4^+CADM1^+$ and $CD4^+CD25^+$ cell fractions in $CD45^+$ peripheral blood lymphocytes from patients with various types of ATLL, HTLV-1 carriers and healthy volunteers. Spearman correlation coefficients were calculated to assess the association between $CD4^+CADM1^+$ and $CD4^+CD25^+$ cell fractions.

The soluble form of CADM1 is detected in the serum of ATLL patients

A soluble isoform of CADM1 consisting of the extracellular domain was recently isolated in murine mast cells.[23] We determined whether the soluble form of CADM1 was present in the serum of ATLL patients by western blot using a chicken anti-human CADM1 antibody. As a positive control, soluble CADM1 was produced by transfection of 293 cells with a construct encoding a soluble form of CADM1 (1 to 374 aa). The soluble CADM1 band (72 kDa) and the recombinant soluble form of CADM1 were clearly detected in the sera of five patients with acute-type ATLL but not in the sera of five healthy volunteers (Figure 4a). We screened the sera of 5 healthy controls and 25 ATLL patients (14 acute-type, 7 lymphoma-type, 2 smoldering-type and 2 HTLV-1 carrier) for the presence of soluble CADM1. We detected different levels of soluble CADM1 among these ATLL patients by western blot (data not shown). In addition, we compared the levels of soluble CADM1 in the serum and the percentages of $CD4^+CADM1^+$ cells in the peripheral blood (Supplementary Figure 4) and confirmed that high levels of soluble CADM1 are present in the serum of patients who had high numbers of $CADM1^+$ cells in the peripheral blood. As serum levels of soluble IL-2Rα are correlated with the prognosis

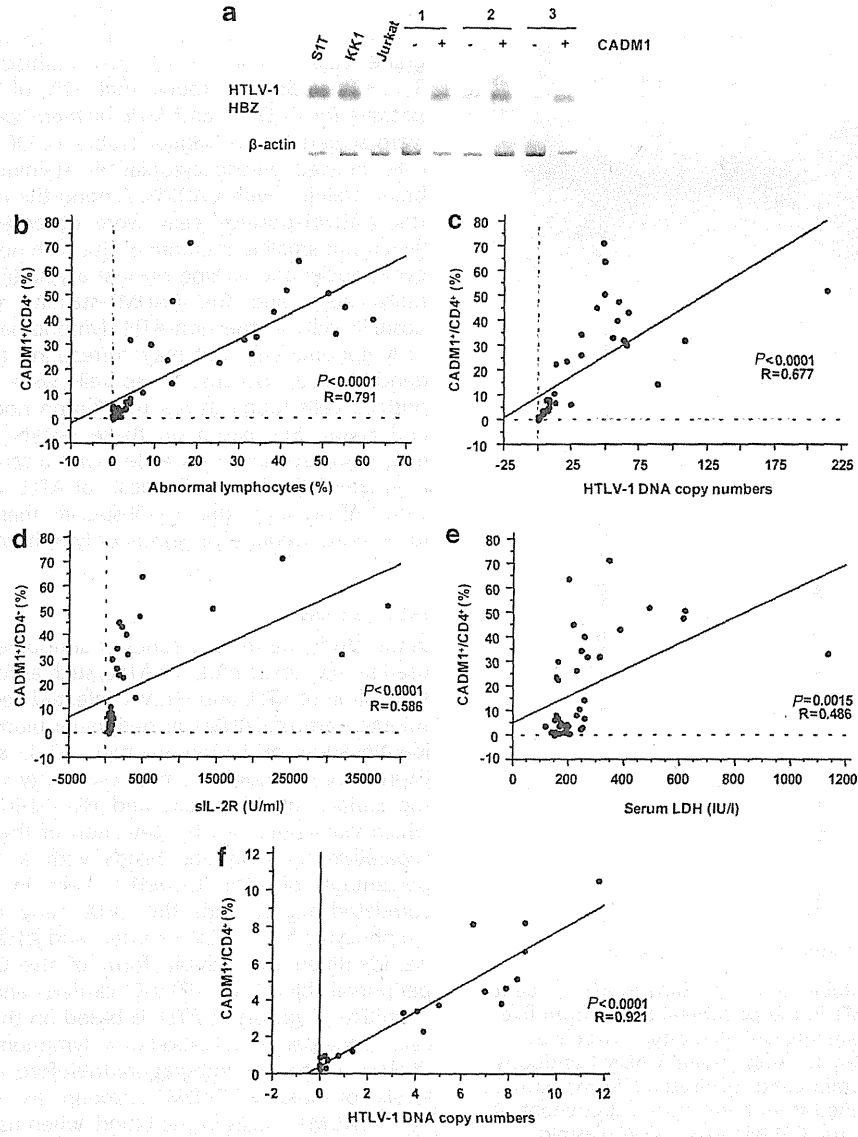

Figure 3. Correlation of the percentages of the $CD4^+CADM1^+$ fraction with the percentages of abnormal lymphocytes, HTLV-1 DNA copy number and the levels of soluble IL-2Rα and serum LDH in both various types of patients with ATLL and HTLV-1 carriers. (**a**) Identification of the HTLV-1 genome by PCR amplification after separation by CADM1-magnetic beads. After separation of the peripheral blood of three ATLL patients by magnetic beads, genomic DNA was extracted from both the CADM1 and non-CADM1 fractions and amplified by specific PCR primers for HTLV-1 *HBZ*. Two ATLL cell lines (S1T and KK1) were used as positive controls, and a T-ALL cell line (Jurkat) was used as a negative control for the HTLV-1 *HBZ*. Lane 1, smoldering ATLL; lane 2, chronic ATLL; lane 3, HTLV-1 carrier. (**b-e**) The percentage of the $CD4^+CADM1^+$ fraction was compared with the percentage of abnormal lymphocytes, the HTLV-1 DNA copy number and the levels of soluble IL-2Rα and serum LDH in both various types of patients with ATLL and HTLV-1 carriers. In (**d**), data from one acute-type patient were not included in the analysis because of the extremely high levels of soluble IL-2Ra ($CD4^+CADM1^+$, 32.9%; IL-2Ra, 96 900 U/ml). (**f**) The percentage of the $CD4^+CADM1^+$ fraction was compared with the HTLV-1 DNA copy number in HTLV-1 carriers.

of ATLL patients, we compared the serum levels of soluble CADM1 and soluble IL-2Rα in individual cases. As shown in Figure 4b, significantly higher levels of soluble CADM1 were detected in the serum of ATLL patients who had increased levels of soluble IL-2Rα; thus, serum CADM1 levels may be a diagnostic tool for the prediction of disease progression in ATLL.

High expression of CADM1 in ATLL-derived lymphomas

To examine the expression of CADM1 in tissue sections from lymphoma-type ATLL, formalin-fixed lymphoma samples from different types of malignant lymphomas were immunostained with the anti-CADM1 antibody. For these studies, we used a monoclonal antibody (1-10C) raised against the recombinant extracellular domain of the CADM1 protein. To confirm the reactivity of the anti-CADM1 antibody in formalin-fixed ATLL cells, cell pellets from various leukemia cell lines were fixed in 10% formalin, embedded in paraffin and stained for CADM1. The anti-CADM1 antibody specifically stained the surface of the CADM1-positive S1T-ATLL cell line but did not react with the CADM1-negative ED-ATLL and all non-ATLL cell lines (Figure 5a, panels 1 and 2, and Supplementary Figure 5a). Western blot analysis confirmed the lack of CADM1 expression in these cell lines (Figure 1a and Supplementary Figure 5b). We next performed immunostaining of lymph node biopsies from ATLL patients with malignant lymphoma using the anti-CADM1 antibody. As positive controls, we used erythrocytes and peripheral nerve tissue (Figure 5a, panels 3 and 4).[17,18] In addition, we examined CADM1

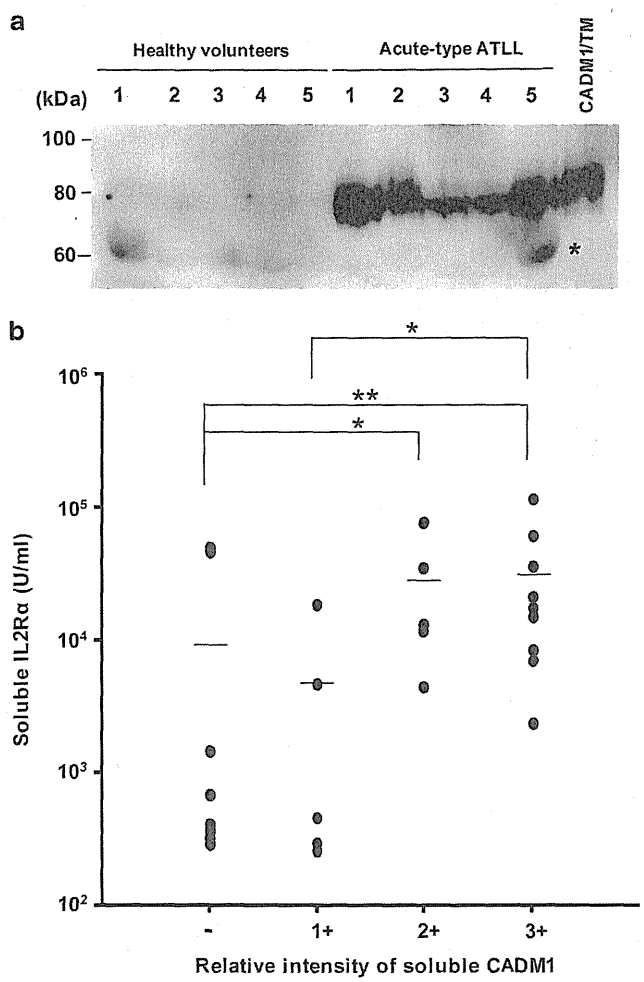

Figure 4. Identification of a soluble form of CADM1 in ATLL patients. (**a**) The soluble form of CADM1 in the peripheral blood from five healthy volunteers and five patients with acute-type ATLL was identified by immunoblot analysis using an anti-CADM1 antibody. The asterisk indicates an albumin band. Truncated CADM1 with an extracellular domain was purified from the culture supernatant of 293 cells after transfection of the CADM1 expression plasmid as a positive control. (**b**) The relative band intensity of CADM1 by immunoblot was compared with the level of sIL-2Rα in various serum samples from healthy volunteers, HTLV-1 carriers and ATLL patients. The band intensity was measured by the Image Gauge software (Fujifilm, Tokyo, Japan). The signal intensities were classified as either high (3+), medium (2+), low (1+) or undetectable (-). Asterisks indicate a significant difference between the band intensities of the groups (*$P<0.001$, **$P<0.0001$).

expression in three cases of lymph nodes with reactive follicular and/or paracortical hyperplasia (reactive lymph nodes) and found that most of the lymphocytes in the reactive lymph nodes were negatively stained and <1% of the cells were positively stained (Figure 5a, panel 5). The staining pattern of the CADM1-positive cells in the reactive lymph nodes mainly shows a uniform cytoplasmic pattern rather than the specific membranous staining that was seen in ATLL cells (as shown below and in Figure 1b). The CADM1-positive cells in reactive lymph node possibly correspond to histiocytes, including dendritic cells because a subset of T-cell zone dendritic cells was reported to express CADM1 (Necl-2) within the lymph node.[24,25] We examined 90 tissue samples from patients with various types of lymphoma, including 36 patients with ATLL and 54 with non-ATLL lymphomas, using erythrocytes and nerve fascicles as positive controls. Of the non-ATLL samples, 29 cases were T- or NK-cell lymphomas, 37 cases were B-cell lymphomas and 2 cases were null-cell lymphomas. Using a four-grade scale to score CADM1 immunohistochemical staining (0 to 3+, Figure 5b), we found that 92% of ATLL lymphomas were positive for CADM1, and 50% of them were heavily stained and were scored 2+ or higher (Table 1). Of note, a few lymphoma cells showed diffuse cytoplasmic staining in addition to membrane staining with CADM1. Among the non-ATLL lymphomas, a few CADM1-positive cells were observed, the morphology of which was small to medium in size with normochromatic round to ovoid nuclei and lacking nuclear atypia (Figure 5c). Based on the morphology and the CADM1-staining patterns, the CADM1-positive cells in the non-ATLL lymphomas were not considered as lymphoma cells but may correspond to histiocytes, including dendritic cells, because these cells were similar to the CADM1-positive cells found in reactive lymph nodes (Figure 5a, panel 5 and Figure 5c). Based on these results, a high degree of cell membrane staining for CADM1 with a score of 2+ may provide high specificity in the diagnosis of ATLL, and combined staining with CADM1 and other T-cell-specific markers may be necessary for a more accurate diagnosis of lymphoma-type ATLL.

DISCUSSION

In this study, we made a series of antibodies against CADM1 to be used as diagnostic tools for ATLL, such as for the identification and separation of ATLL and HTLV-1-infected cells, the detection of the soluble form of CADM1 in peripheral blood and the pathological identification of lymphoma-type ATLL after formalin fixation. Expression of CADM1 by flow cytometry was clearly detected on the surface of ATLL cells and HTLV-1-infected T lymphocytes, which was confirmed by detection of the HTLV-1 genome after separation by magnetic beads with a CADM1 antibody. The percentage of $CD4^+CADM1^+$ cells in the peripheral blood correlated highly with the DNA copy number of HTLV-1 in lymphocytes from HTLV-1 carriers and ATLL patients. In particular, we identified the soluble form of the CADM1 protein in the peripheral blood of HTLV-1 carriers and ATLL patients. The definitive diagnosis of ATLL is based on the confirmation of ATLL cells in the peripheral blood or in lymphoma tumors by detection of HTLV-1 genomic integration; therefore, measurement of serum levels of soluble CADM1 protein as well as detection of $CD4^+CADM1^+$ cells in the blood, when used in conjunction with other standard diagnostic methods, would be useful for identifying and monitoring disease progression in HTLV-1 carriers with increased accuracy and may aid in the early diagnosis and measurement of treatment effects for ATLL.

It has been proposed that HTLV-1 infects various types of cells, including T-reg cells and subsets of T helper cells (Th2 and Th17), in a cell-to-cell manner.[26–29] There is also evidence that ATLL cells act as T-reg cells that express CD4, CD25 and FoxP3 and are thought to contribute to the immune suppression of ATLL patients;[6] however, it was reported that CADM1 is expressed at low levels on resting naive T cells, and its expression is further downregulated 14 h following TCR activation.[30] Therefore, we determined the expression of CADM1 in the T-reg cell fraction of the peripheral blood of healthy volunteers. The results showed that a subset of the T-reg fraction weakly expressed CADM1, suggesting that CADM1 is not a major marker for the T-reg fraction and that CADM1 expression on ATL cells may reflect the fact that ATL cells originate from T-reg cells. As ATLL cells that constitutively express CD25 exhibited heterogeneous Foxp3 expression patterns,[5] a part of ATLL is likely derived from $FoxP3^+$ T-reg cells. In another report, a population of $FoxP3^+$ cells distinct from ATLL cells was shown to have a regulatory function and was found to impair the cell-mediated immune response to HTLV-1 in patients with ATLL.[31] Although we do not know whether the population of T-reg cells with weak expression of CADM1 in the

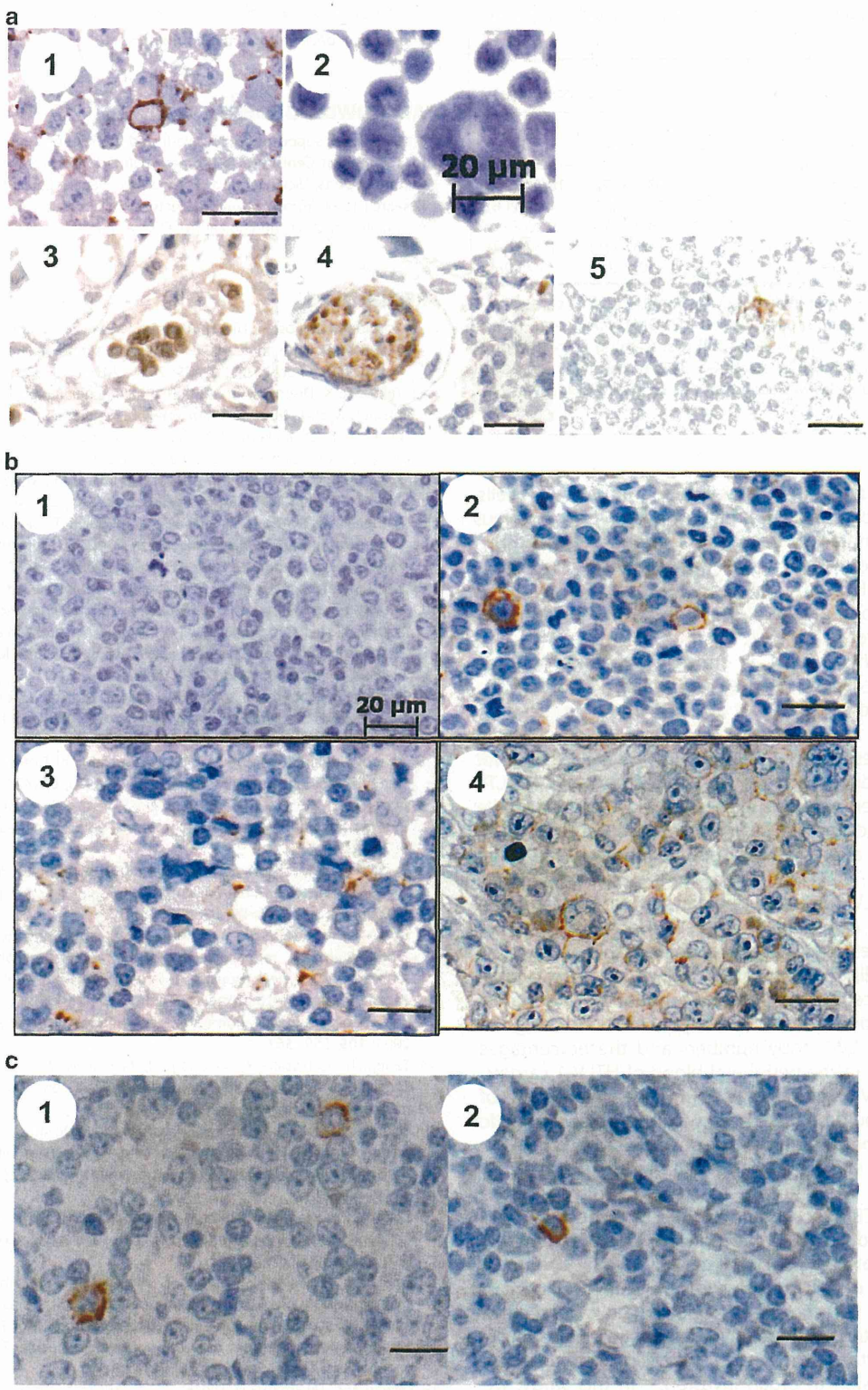

Figure 5. Expression of CADM1 in lymphoma-type ATLL. (**a**) Immunostaining of CADM1 in the S1T-ATLL cell line was used as a positive control (a1), and the ED-ATLL cell line was used as a negative control (a2) for CADM1 expression using an anti-CADM1 antibody (1-10C). Immunostaining of erythrocytes in the blood vessels (**c**), peripheral nerve cells (a3) and reactive lymph nodes (a4) using the same antibody. Scale bar, 20 μm. (**b**) The immunoreactivity for CADM1 was scored using a standardized four-tiered scoring scale as follows: staining in >30% of cells was scored as 3+ (b4); staining in >5% but <30% of cells was scored as 2+ (b3); staining in <5% of cells was scored as 1+ (b2); and a lack of staining was scored as 0 (b1). These images were taken from immunostained ATLL lymphoma sections. Scale bar, 20 μm. (**c**) Representative CADM1 immunostaining in B-cell (c1) and NK-cell (c2) lymphomas. Scale bar, 20 μm.

Table 1. Immunohistochemical staining of CADM1 in various types of lymphomas, including ATLL

	Case numbers	Staining scores				Positive rates (%)	
		Negative	1+	2+	3+	⩾1+	⩾2+
ATLL	36	3	15	14	4	33/36 (92)	18/36 (50)
Non-ATLL	54	37	16	1	0	17/54 (31)	1/54 (1.8)
T/NK	15	12	3	0	0	3/15 (20)	0/15 (0)
B	37	23	13	1	0	14/37 (38)	1/37 (2.7)
Null	2	2	0	0	0	0/2 (0)	0/2 (0)

Abbreviations: ATLL, adult T-cell leukemia/lymphoma; CADM1, cell adhesion molecule 1. The immunoreactivity for CADM1 was scored using a standardized four-tiered scoring scale as follows: staining in >30% of cells was scored as 3+; staining in >5% but <30% of cells was scored as 2+; staining in <5% of cells was scored as 1+; lack of staining was scored as 0.

PBMCs of healthy volunteers is the cellular origin for ATLL cells, CADM1 is thought to be one of the major markers for the various types of ATLL cells. In fact, we observed strong expression of CADM1 in rare cases of ATLL characterized by the $CD4^+CD8^+$, $CD4^-CD8^+$ or $CD4^-CD8^-$ phenotypes (data not shown); therefore, the $CADM1^{high}$ population of T-lymphocytes in peripheral blood can be considered ATLL cells.

The question of why CADM1 is strongly expressed on the surface of various types of ATLL remains unclear. Previously, we investigated whether the expression of CADM1 was induced by HTLV-1/Tax expression and found that Tax protein expression did not activate the expression of CADM1 in JPX-9 cells (data not shown). We also introduced a Tax expression vector into MOLT4 and 293T cells and determined the expression level of CADM1. We found that Tax could not induce CADM1 expression in these cells, suggesting that Tax expression is not related to the high expression of CADM1. As HBZ is known to be constitutively expressed in both HTLV-1-infected cells and ATLL cells and can modulate transcription of cellular genes,[16] it is possible that HBZ activates CADM1 expression. We also speculate that $CADM1^{high}$ expression in ATLL cells may be associated with transcriptional abnormalities in ATLL cells through the accumulation of genomic or epigenomic alterations. In this study, we found a good correlation between HTLV-1 copy numbers and the percentages of $CD4^+CADM1^+$ cells in the peripheral blood of HTLV-1 carriers, suggesting that HTLV-1 carriers with high percentages of $CD4^+CADM1^+$ cells could be associated with progressive genetic alterations and might be at high risk for developing ATLL.

Recent studies have shown that a few markers, such as CCR4 and CD70, are unique ATLL surface markers.[32,33] Although the proportion of $CD4^+CCR4^+$ cells and $CD4^+CD70^+$ cells in the PBMCs from healthy individuals were found to be approximately 5%,[27,33] the proportion of $CD4^+CADM1^+$ cells was <1% (Figure 2); therefore, measurement of $CADM1^+$ T cells is particularly efficient in the diagnosis of HTLV-1 infection in individuals who carry a small number of HTLV-1-infected cells. We have demonstrated previously that CADM1 has important functions in increasing cell adhesion and mediating progression to organ invasion.[19] In this study, we succeeded in isolating a low percentage of both HTLV-1-infected cells from the PBMCs of HTLV-1 carriers with high HTLV-1 copy numbers and ATLL cells from patients with ATLL. The sorted HTLV-1-infected cells and ATLL cells could become useful tools for transcriptional and/or genomic analysis that may be used to compare their results with those of PBMCs from either healthy volunteers or peripheral leukemia cells from patients with ATLL. The results may provide important information on the expression patterns and/or genomic abnormalities that occur at the early stages of HTLV-1 infection and/or ATLL development.

CONFLICT OF INTEREST

The authors declare no conflict of interest.

ACKNOWLEDGEMENTS

This work was supported by Grants-in-Aid for Scientific Research of Priority Area and for twenty-first Century COE program (Life science) from the Ministry of Education, Culture, Sports, Science and Technology, Japan Leukemia Research fund, and Research fund from Miyazaki Prefecture Collaboration of Regional Entities for the Advancement of Technological Excellence, JST.

REFERENCES

1 Yoshida M, Miyoshi I, Hinuma Y. Isolation and characterization of retrovirus from cell lines of human adult T-cell leukemia and its implication in the disease. *Proc Natl Acad Sci USA* 1982; **79**: 2031-2035.
2 Takatsuki K. Discovery of adult T-cell leukemia. *Retrovirology* 2005; **2**: 16.
3 Arisawa K, Soda M, Endo S, Kurokawa K, Katamine S, Shimokawa I *et al.* Evaluation of adult T-cell leukemia/lymphoma incidence and its impact on non-Hodgkin lymphoma incidence in southwestern Japan. *Int J Cancer* 2000; **85**: 319-324.
4 Proietti FA, Carneiro-Proietti AB, Catalan-Soares BC, Murphy EL. Global epidemiology of HTLV-I infection and associated diseases. *Oncogene* 2005; **24**: 6058-6068.
5 Karube K, Ohshima K, Tsuchiya T, Yamaguchi T, Kawano R, Suzumiya J *et al.* Expression of FoxP3, a key molecule in CD4CD25 regulatory T cells, in adult T-cell leukaemia/lymphoma cells. *Br J Haematol* 2004; **126**: 81-84.
6 Chen S, Ishii N, Ine S, Ikeda S, Fujimura T, Ndhlovu LC *et al.* Regulatory T cell-like activity of Foxp3+ adult T cell leukemia cells. *Int Immunol* 2006; **18**: 269-277.
7 Yasuda N, Lai PK, Ip SH, Kung PC, Hinuma Y, Matsuoka M *et al.* Soluble interleukin 2 receptors in sera of Japanese patients with adult T cell leukemia mark activity of disease. *Blood* 1988; **71**: 1021-1026.
8 Kamihira S, Atogami S, Sohda H, Momita S, Yamada Y, Tomonaga M. Significance of soluble interleukin-2 receptor levels for evaluation of the progression of adult T-cell leukemia. *Cancer* 1994; **73**: 2753-2758.
9 Akagi T, Ono H, Shimotohno K. Characterization of T cells immortalized by Tax1 of human T-cell leukemia virus type 1. *Blood* 1995; **86**: 4243-4249.
10 Furukawa Y, Kubota R, Tara M, Izumo S, Osame M. Existence of escape mutant in HTLV-I tax during the development of adult T-cell leukemia. *Blood* 2001; **97**: 987-993.
11 Tamiya S, Matsuoka M, Etoh K, Watanabe T, Kamihira S, Yamaguchi K *et al.* Two types of defective human T-lymphotropic virus type I provirus in adult T-cell leukemia. *Blood* 1996; **88**: 3065-3073.
12 Koiwa T, Hamano-Usami A, Ishida T, Okayama A, Yamaguchi K, Kamihira S *et al.* 5'-long terminal repeat-selective CpG methylation of latent human T-cell leukemia virus type 1 provirus *in vitro* and *in vivo*. *J Virol* 2002; **76**: 9389-9397.
13 Takeda S, Maeda M, Morikawa S, Taniguchi Y, Yasunaga J, Nosaka K *et al.* Genetic and epigenetic inactivation of tax gene in adult T-cell leukemia cells. *Int J Cancer* 2004; **109**: 559-567.
14 Taniguchi Y, Nosaka K, Yasunaga J, Maeda M, Mueller N, Okayama A *et al.* Silencing of human T-cell leukemia virus type I gene transcription by epigenetic mechanisms. *Retrovirology* 2005; **2**: 64.
15 Basbous J, Arpin C, Gaudray G, Piechaczyk M, Devaux C, Mesnard JM. The HBZ factor of human T-cell leukemia virus type I dimerizes with transcription factors JunB and c-Jun and modulates their transcriptional activity. *J Biol Chem* 2003; **278**: 43620-43627.
16 Satou Y, Yasunaga J, Yoshida M, Matsuoka M. HTLV-I basic leucine zipper factor gene mRNA supports proliferation of adult T cell leukemia cells. *Proc Natl Acad Sci USA* 2006; **103**: 720-725.
17 Sasaki H, Nishikata I, Shiraga T, Akamatsu E, Fukami T, Hidaka T *et al.* Overexpression of a cell adhesion molecule, TSLC1, as a possible molecular marker for acute-type adult T-cell leukemia. *Blood* 2005; **105**: 1204-1213.
18 Murakami Y. Involvement of a cell adhesion molecule, TSLC1/IGSF4, in human oncogenesis. *Cancer Sci* 2005; **96**: 543-552.
19 Dewan MZ, Takamatsu N, Hidaka T, Hatakeyama K, Nakahata S, Fujisawa J *et al.* Critical role for TSLC1 expression in the growth and organ infiltration of adult T-cell leukemia cells *in vivo*. *J Virol* 2008; **82**: 11958-11963.
20 Tanaka G, Okayama A, Watanabe T, Aizawa S, Stuver S, Mueller N *et al.* The clonal expansion of human T lymphotropic virus type 1-infected T cells: a comparison between seroconverters and long-term carriers. *J Infect Dis* 2005; **191**: 1140-1147.
21 Shimizu Y, Takamori A, Utsunomiya A, Kurimura M, Yamano Y, Hishizawa M *et al.* Impaired Tax-specific T-cell responses with insufficient control of HTLV-1 in a subgroup of individuals at asymptomatic and smoldering stages. *Cancer Sci* 2009; **100**: 481-489.
22 Kurosawa G, Akahori Y, Morita M, Sumitomo M, Sato N, Muramatsu C *et al.* Comprehensive screening for antigens overexpressed on carcinomas via

isolation of human mAbs that may be therapeutic. *Proc Natl Acad Sci USA* 2008; **105**: 7287-7292.
23 Koma Y, Ito A, Wakayama T, Watabe K, Okada M, Tsubota N *et al.* Cloning of a soluble isoform of the SgIGSF adhesion molecule that binds the extracellular domain of the membrane-bound isoform. *Oncogene* 2004; **23**: 5687-5692.
24 Galibert L, Diemer GS, Liu Z, Johnson RS, Smith JL, Walzer T *et al.* Nectin-like protein 2 defines a subset of T-cell zone dendritic cells and is a ligand for class-I-restricted T-cell-associated molecule. *J Biol Chem* 2005; **280**: 21955-21964.
25 Takeuchi A, Itoh Y, Takumi A, Ishihara C, Arase N, Yokosuka T *et al.* CRTAM confers late-stage activation of CD8+ T cells to regulate retention within lymph node. *J Immunol* 2009; **183**: 4220-4228.
26 Imai T, Nagira M, Takagi S, Kakizaki M, Nishimura M, Wang J *et al.* Selective recruitment of CCR4-bearing Th2 cells toward antigen-presenting cells by the CC chemokines thymus and activation-regulated chemokine and macrophage-derived chemokine. *Int Immunol* 1999; **11**: 81-88.
27 Baatar D, Olkhanud P, Sumitomo K, Taub D, Gress R, Biragyn A. Human peripheral blood T regulatory cells (Tregs), functionally primed CCR4+ Tregs and unprimed CCR4- Tregs, regulate effector T cells using FasL. *J Immunol* 2007; **178**: 4891-4900.
28 Lim HW, Lee J, Hillsamer P, Kim CH. Human Th17 cells share major trafficking receptors with both polarized effector T cells and FOXP3+ regulatory T cells. *J Immunol* 2008; **180**: 122-129.
29 Hieshima K, Nagakubo D, Nakayama T, Shirakawa AK, Jin Z, Yoshie O. Tax-inducible production of CC chemokine ligand 22 by human T cell leukemia virus type 1 (HTLV-1)-infected T cells promotes preferential transmission of HTLV-1 to CCR4-expressing CD4+ T cells. *J Immunol* 2008; **180**: 931-939.
30 Yeh JH, Sidhu SS, Chan AC. Regulation of a late phase of T cell polarity and effector functions by Crtam. *Cell* 2008; **132**: 846-859.
31 Toulza F, Nosaka K, Takiguchi M, Pagliuca T, Mitsuya H, Tanaka Y *et al.* FoxP3+ regulatory T cells are distinct from leukemia cells in HTLV-1-associated adult T-cell leukemia. *Int J Cancer* 2009; **125**: 2375-2382.
32 Yoshie O, Fujisawa R, Nakayama T, Harasawa H, Tago H, Izawa D *et al.* Frequent expression of CCR4 in adult T-cell leukemia and human T-cell leukemia virus type 1-transformed T cells. *Blood* 2002; **99**: 1505-15011.
33 Baba M, Okamoto M, Hamasaki T, Horai S, Wang X, Ito Y *et al.* Highly enhanced expression of CD70 on human T-lymphotropic virus type 1-carrying T-cell lines and adult T-cell leukemia cells. *J Virol* 2008; **82**: 3843-3852.

Supplementary Information accompanies the paper on the Leukemia website (http://www.nature.com/leu)

J Clin Exp Hematopathol
Vol. 52, No. 1, May 2012

Review Article

CADM1/TSLC1 is a Novel Cell Surface Marker for Adult T-Cell Leukemia/Lymphoma

Shingo Nakahata and Kazuhiro Morishita

CADM1/TSLC1 (Cell adhesion molecule 1/Tumor suppressor in lung cancer 1) is a cell adhesion molecule that was originally identified as a tumor suppressor in lung cancer. *CADM1/TSLC1* expression is reduced in a variety of cancers via promoter methylation, and this reduction is associated with poor prognosis and enhanced metastatic potential. In contrast, we observed that *CADM1/TSLC1* is highly and ectopically expressed in all primary adult T-cell leukemia/lymphoma (ATLL) cells and in most human T-cell leukemia virus type (HTLV)-1-infected T-cell and ATLL cell lines. No expression, however, was detected in $CD4^+$ T cells or in several other non-HTLV-1-infected leukemia cells. Moreover, we identified that high CADM1/TSLC1 expression plays an important role in enhanced cell-cell adhesion to the vascular endothelium, tumor growth and the ability of ATLL cells to infiltrate organs. We developed various antibodies as diagnostic tools to identify $CADM1^+$ ATLL cells. Using flow cytometry, we determined that CADM1/TSLC1 is present on the surface of ATLL cells. The percentage of $CD4^+$ $CADM1^+$ cells in the peripheral blood of HTLV-1 carriers and ATLL patients was highly correlated with the DNA copy number of HTLV-1 in lymphocytes. In particular, we identified the soluble form of CADM1/TSLC1 in the peripheral blood of HTLV-1 carriers and ATLL patients. Therefore, measurements of soluble CADM1/TSLC1 serum levels and the detection of $CD4^+$ $CADM1^+$ cells in the blood, when combined with standard diagnostic methods, would be useful for identifying and monitoring disease progression in HTLV-1 carriers. Such tests would provide increased accuracy and may aid in early diagnosis and in determining the effects of ATLL treatments. [*J Clin Exp Hematopathol 52(1) : 17-22, 2012*]

Keywords: CADM1/TSLC1, cell adhesion molecule, cell surface marker, invasion, adult T-cell leukemia/ lymphoma

INTRODUCTION

The *CADM1 (Cell adhesion molecule 1, Tumor suppressor in lung cancer 1; TSLC1, IgSF4, Necl2, Syncam* or *SgIGSF*) gene encodes an immunoglobulin (Ig) superfamily cell adhesion molecule (IgCAM). *CADM1* is a well-known tumor suppressor gene in a variety of human cancers, particularly those of epithelial cell origin, including liver, pancreatic and prostate cancers. This gene is generally inactivated in these carcinomas via 2 mechanisms; promoter methylation and/or loss of heterozygosity at the gene locus.[1] The *CADM1* gene encodes a 442-amino acid class I membrane protein and contains three Ig loops in the extracellular domain, a transmembrane domain and a short cytoplasmic domain.[2] This primary structure is also observed in IgCAM protein family members, which are referred to as nectins. Although nectins associate with afadin, CADM1/Necl2 (Nectin-like protein 2) does not.[3] However, several CADM1/TSLC1-interacting proteins have been identified, such as DAL-1/4.1B of the protein 4.1 family, the members of which are known to be spectrin-actin-binding proteins.[4] CADM1/TSLC1 forms homodimers through *cis* interactions, and these interactions contribute to cell-cell interactions at the lateral membranes of polarized epithelial cells.[5] Class I-restricted T cell-associated molecule (CRTAM), a two Ig domain-bearing surface receptor, was also identified as a CADM1/TSLC1 ligand.[6] CADM1/TSLC1 interacts with CRTAM to promote natural killer (NK) cell cytotoxicity, interferon-γ secretion by $CD8^+$ cells *in vitro* and NK cell-mediated rejection of tumors that express CADM1/TSLC1 *in vivo*.[6] It is proposed that the disruption of cell adhesion via the loss of *CADM1/TSLC1* leads to cancer cell invasion or metastasis.[1] The tumorigenic potential of *CADM1/TSLC1*, which is located on chromosome 11q23, was first reported by Murakami *et al.*[7,8] This gene was identified as a tumor suppressor in human non-small-cell lung cancers (NSCLCs) based on combinatorial analyses of yeast artificial chromosome transfers into human NSCLC cells and a tumorigenicity assay of these modified lines in

Received : January 26, 2012
Accepted : February 8, 2012
Division of Tumor and Cellular Biochemistry, Department of Medical Sciences, Faculty of Medicine, University of Miyazaki, Japan
Address correspondence and reprint request to Kazuhiro Morishita, Division of Tumor and Cellular Biochemistry, Department of Medical Sciences, Faculty of Medicine, University of Miyazaki, 5200 Kihara, Kiyotake, Miyazaki 889-1692, Japan.
E-mail : kmorishi@med.miyazaki-u.ac.jp

nude mice.[7,8] Subsequently, a number of studies reported the loss of CADM1/TSLC1 expression in malignant carcinomas. For example, promoter methylation of *CADM1/TSLC1* was demonstrated in 44% of NSCLCs, 27% of pancreatic cancers, 29% of hepatocellular carcinomas, and 32% of prostate cancers.[8-11] Thus, it was concluded that *CADM1/TSLC1* was a tumor suppressor. On the contrary, our laboratory has reported that CADM1/TSLC1 is overexpressed in adult T-cell leukemia/lymphoma (ATLL) cells and plays a role in oncogenesis.[12] Here, we summarize the findings and significance of this area of research.

IDENTIFICATION OF *CADM1/TSLC1* AS A POSSIBLE MARKER FOR ATLL

ATLL is an aggressive and fatal $CD4^+$ T-cell malignancy that is caused by infection with human T-cell leukemia virus type 1 (HTLV-1).[13,14] HTLV-1 is endemic in the Caribbean basin, southern Japan, central and western Africa. After a long latency period, a fraction of carriers develop ATLL.[15] The lifetime incidence of ATLL among HTLV-1 carriers is estimated to be 2.1% in women and 6.6% in men.[16] Despite improved therapies, ATLL still has a very poor prognosis.

The potent oncoprotein Tax is encoded in the pX region of HTLV-1. Tax activates the transcription of HTLV-1 and cellular genes by cooperating with cellular transcription factors. Tax alters many transcriptional pathways, activating cyclic adenosine monophosphate response element binding protein, activator protein-1, and nuclear factor-κB. Tax also represses p53 and interferes with several cell cycle regulators, including cyclins and CDK inhibitors (p15 and p16).[17] These multiple functions of Tax are believed to be involved in the immortalization of HTLV-1-infected cells.

In contrast, Tax expression is undetectable in approximately 60% of leukemias.[18] There are 3 proposed mechanisms for the inactivation of Tax expression in ATLL cells. First, genetic changes (nonsense mutations and deletion) of the *Tax* gene have been described.[18] Second, the deletion of the 5′ long terminal repeat (LTR) that contains the viral promoter has been implicated in the inactivation of Tax expression.[19] Third, the 5′-LTR can be hypermethylated, leading to promoter inactivation.[20] Because Tax is the major target of cytotoxic T-lymphocytes, a disruption or decrease in Tax expression can facilitate the escape of ATLL cells from the host cytotoxic T-lymphocytes, contributing to the development of ATLL. Alternatively, the 3′ LTR may remain unmethylated and intact in ATLL cells.[21] *HBZ* is transcribed from the minus strand of the provirus using the 3′ LTR as a promoter. It has been reported that *HBZ* is expressed in ATLL cells and promotes ATLL cell proliferation.[22] Considering the long latency period of ATLL, it has been proposed that at least five additional genetic or epigenetic events are required for the development of overt disease.[23] Although no specific chromosomal abnormalities have been identified in ATLL,[24,25] human leukemias are often associated with primary genetic alterations, usually non-random reciprocal chromosomal translocations.[26] It has been reported that the tumor suppressor genes *p53, p15*, and *p16* are disrupted in aggressive ATLL via chromosomal loss or promoter methylation.[27] However, because ATLL-related genomic alterations are enormously diverse and complex, the molecular basis of the multistep process of leukemogenesis in ATLL remains unclear.

To identify specific genetic markers for ATLL, we previously described the gene expression profiles of ATLL cells and identified highly expressed genes therein. These analyses were performed using cells from patients with acute-type ATLL using a GeneChip microarray, which contained oligonucleotide hybridization probes for more than 12,000 genes.[12] After determining the expression profiles from the panels of ATLL patients, we identified three genes that were upregulated more than 30-fold in ATLL cells, including *CADM1/TSLC1*, *caveolin 1* (*CAV1*), and *prostaglandin D2 synthase*. Unexpectedly, *CADM1/TSLC1* was overexpressed in all primary ATLL cells and in most HTLV-1-infected T-cells and ATLL cell lines. As described above, CADM1/TSLC1 is a member of the Ig superfamily of cell adhesion molecules and participates in cell-cell interactions. Previous reports have demonstrated that CADM1/TSLC1 is expressed in nearly all organs but not in lymphoid tissues,[2] suggesting a functional role in epithelial cell adhesion. In our studies of a series of hematopoietic cells, CADM1/TSLC1 was weakly expressed in erythrocytes, to a lower degree by neutrophils, monocytes, and B cells and was not expressed in T cells. The activation of T cells with PHA or an anti-CD3 and anti-CD28 antibody mixture did not induce CADM1/ TSLC1 expression, indicating that the CADM1/TSLC1 expression in ATLL cells did not result from the activation of normal T cells. Moreover, CADM1/TSLC1 expression was not detected in 34 HTLV-1-uninfected leukemia cell lines, consisting of 17 myelocytic/monocytic, 3 megakaryocytic, 2 erythrocytic, 4 B-lymphocytic, and 8 T-lymphocytic leukemia cell lines.[12] These findings suggest that TSLC1 is specifically expressed in ATLL and HTLV-1-infected T cells.

PHYSIOLOGICAL ROLES OF CADM1/TSLC1 IN ATLL CELLS

One characteristic feature of ATLL cases is the invasion of the lymph nodes, skin, or various other organs by malignant cells. When the ED-ATLL cell line, which expresses very low CADM1/TSLC1 levels, was stably transfected with a CADM1 vector and assayed for self-aggregation ability, ED/CADM1 cells were found to form aggregates within 30 minutes. In contrast, parental ED cells or ED/neo cells exhibited little aggregation in this time period,[12] suggesting that

CADM1/TSLC1 mediates the intercellular adhesion of ATLL cells via homophilic interactions. However, the potential *in vivo* pathologic significance of this self-aggregation of ATLL cells is unclear. The initial step in the invasion of various human organs by ATLL cells is their interaction with vascular endothelial cells.[28] Therefore, we examined the possible involvement of CADM1/TSLC1 in the adhesion of ATLL cells to human umbilical vein endothelial cells (HUVECs) *in vitro*.[12] When fluorescence-labeled ED cells and their derivatives were seeded onto HUVECs, incubated for 30 minutes, and then washed with medium, the numbers of attached ATLL cells was significantly (3-fold) higher in ED/CADM1 cells compared with parental ED or ED/neo cells. These results suggest that ectopic CADM1/TSLC1 expression in ATLL cells may promote their invasion of various organs via an interaction with the surface molecules of vascular endothelial cells.

CRITICAL ROLE OF *CADM1/TSLC1* IN THE GROWTH AND ORGAN INFILTRATION OF ATLL CELLS

We examined the role of CADM1/TSLC1 in the growth and infiltration of leukemia cells using C57BL/6J and NOD-SCID/γc^{null} (NOG) mice.[29] First, a murine IL-2-independent T-lymphoma cell line (EL4) was intraperitoneally injected into syngeneic C57BL/6J mice as a model for ATLL. The EL4/CADM1 mice died significantly earlier than the control mice. Massive tumor metastasis was evident in the livers of the mice that were injected with EL4/CADM1 cells. These results indicate that CADM1/TSLC1 overexpression in T-lymphoma cells aggressively promotes the development of leukemia/ lymphoma. Next, ATLL-derived ED cells were subcutaneously injected into NOG mice. The ED/CADM1 cell lines caused greater formation of larger tumors than did the ED/Neo and parental cell lines. Clinical signs of being near death (e.g., piloerection, weight loss, and cachexia) at the time of sacrifice were more prevalent in those mice that were injected with the ED/CADM1 cell line. These results suggest that CADM1/TSLC1 expression in ATLL cells enhances *in vivo* tumor growth in NOG mice. Because the mice died within 4 weeks due to heavy tumor burden following subcutaneous inoculation of leukemia cells, ED/CADM1 or ED/Neo cells were intravenously injected into NOG mice to investigate their capacity to invade various organs. Macroscopically, all of the mice injected with ED/CADM1 cells (six/six) exhibited severe liver invasion with ovarian swelling. None of the mice injected with ED/Neo cells exhibited liver invasion but did demonstrate ovarian involvement. Microscopically, all of the mice that were inoculated with ED/CADM1 cells exhibited severe and massive liver and lung invasions. Alternatively, only one of the six mice that were inoculated with ED/Neo cells exhibited a sizable liver metastasis. Thus, CADM1/TSLC1 overexpression in ATLL cells may enhance organ invasion, particularly that of the liver and lung. Finally, we have shown that primary ATLL cells with high CADM1/TSLC1 expression levels can efficiently grow and infiltrate various organs in NOG mice.[29] Primary CADM1$^+$ ATLL cells, with various CADM1/TSLC1 expression levels, from five acute-type and five chronic-type ATLL patients were subcutaneously inoculated into the postauricular region of NOG mice. All of the mice exhibited clinical signs of being near death (e.g., piloerection, weight loss, and cachexia) 6 to 8 weeks following the inoculation. These mice also exhibited enlarged lymph nodes, spleens, lungs, and livers. Microscopically, the ATLL cells invaded various organs to different degrees in all of the ATLL-bearing NOG mice. The dispersion diagram for the levels of invasion and the cellular CADM1/TSLC1 expression levels revealed a correlation coefficient of 0.714, suggesting that there was a moderate correlation between the invasive capability of the cells and the CADM1/TSLC1 expression level. Thus, CADM1/TSLC1 aided in the formation of a rapidly growing large tumor and massive infiltration of ATLL cells into various organs in NOG mice. Because CADM1/TSLC1 is expressed in various ATLL types, including smoldering and chronic types, this gene may be a promising target for the development of a novel ATLL therapy. The NOG mouse model system described here may provide a novel means by which to understand and further investigate the importance of CADM1 in ATLL progression.

CLINICAL SIGNIFICANCE OF *CADM1/TSLC1* EXPRESSION IN ATLL

The determination of clonal HTLV-1 proviral integration by Southern blot analysis is the gold standard for a definitive ATLL diagnosis. In addition, the presence of leukemia cells with multi-lobulated nuclei (referred to as "flower cells") in the peripheral blood is a morphologic characteristic feature of ATLL. Hypercalcemia and high levels of either serum lactate dehydrogenase (LDH) or soluble IL-2Ra (sIL-2Rα) have been demonstrated to be unfavorable markers for ATLL ; however, these markers are not specific for the diagnosis of ATLL.[30,31] Recently, we generated a series of antibodies against CADM1/TSLC1 to be used as diagnostic tools for ATLL. These antibodies can be used for the identification and separation of ATLL and HTLV-1-infected cells, the detection of the soluble form of CADM1/TSLC1 in the peripheral blood and the pathological identification of lymphoma-type ATLL following formalin fixation.[32,33]

CADM1/TSLC1 expression in leukemia cells from ATLL patients and from HTLV-1-infected cells from viral carriers

ATLL cells exhibit an activated helper T-cell profile (i.e.,

$CD3^+$, $CD4^+$, $CD8^-$, and $CD25^+$). It was reported that 10 of 17 ATLL cases (59%) expressed forkhead box P3, the expression of which is characteristic of $CD4^+$ and $CD25^+$ regulatory T (T-reg) cells.[34] These data suggest that certain ATLL cases originate from T-reg cells. Interestingly, we observed, using flow cytometric analysis, that a subset of the T-reg fraction weakly expressed CADM1/TSLC1, suggesting that CADM1/TSLC1 is not a major marker for the T-reg fraction and that CADM1/TSLC1 expression on ATLL cells may reflect their T-reg cell origin.[33] Among $CD45^+$ cells in PBMCs from healthy volunteers, 7.3% of $CD45^+$ cells also expressed CD4 and CD25, while only 0.6% of the cell population expressed CD4 and CADM1/TSLC1. These results indicate that the number of $CD4^+CADM1^+$ cells was significantly lower than the number of $CD4^+CD25^+$ cells in healthy volunteer PBMCs. The median percentages of $CD4^+CADM1^+$ cells were 73.9% in acute cases, 72.4% in chronic cases, 5.6% in lymphoma cases, 11.5% in smoldering cases and 4.4% in HTLV-1 carriers. The percentages of $CD4^+CD25^+$ cells were significantly correlated with those of $CD4^+CADM1^+$ cells ($R = 0.907$, $P < 0.0001$), suggesting that the majority of the ATLL cells were $CD4^+CD25^+CADM^+$. The percentages of $CD4^+CADM1^+$ cells exhibited a high degree of correlation with both the percentage of abnormal lymphocytes ($R = 0.791$, $P < 0.0001$) and with the HTLV-1 DNA copy number ($R = 0.677$, $P < 0.0001$) in various ATLL types. In addition, the percentages of $CD4^+CADM1^+$ cells were correlated with sIL-2R*a* and LHD levels ($R = 0.586$, $P < 0.0001$ and $R = 0.486$, $P = 0.0015$, respectively). To further evaluate the diagnostic efficacy of $CADM1^+$ cell numbers in detecting HTLV-1-infected cells, the HTLV-1 provirus copy number was compared with the percentages of $CD4^+CADM1^+$ cells and sIL-2Ra and LDH serum levels in carrier PBMCs. The percentage of $CD4^+CADM1^+$ cells exhibited a significant correlation with the HTLV-1 DNA copy number ($R = 0.921$, $P < 0.0001$), whereas a poor correlation was observed between the HTLV-1 copy number and sIL-2Ra and LDH levels. Based on these data, in addition to the determination of HTLV-1 proviral DNA copy number, the quantification of $CD4^+CADM1^+$ cell number by flow cytometry may be useful with respect to monitoring the number of HTLV-1-infected cells in the peripheral blood of ATLL patients and HTLV-1 carriers.

Detection of the soluble form of CADM1/TSLC1 in the serum of ATLL patients

A soluble CADM1/TSLC1 isoform consisting of the extracellular domain was recently isolated in murine mast cells.[35] Using western blot analysis, we observed a 72-kDa soluble CADM1/TSLC1 protein in the sera of 5 patients with acute-type ATLL but not in the sera of 5 healthy volunteers. The analysis of the sera of 5 healthy controls and of 25 ATLL patients (14 acute-type, 7 lymphoma-type, 2 smoldering-type and 2 HTLV-1 carriers) revealed that high levels of soluble CADM1/TSLC1 were present in the serum of patients who had high numbers of $CADM1^+$ cells in the peripheral blood. Furthermore, when comparing the soluble IL-2Ra and CADM1/TSLC1 serum levels in individual cases, significantly higher levels of soluble CADM1/TSLC1 were detected in the serum of ATLL patients who had increased levels of soluble IL-2Ra ; thus, serum CADM1/TSLC1 levels may be predictive of disease progression in ATLL.[33]

High CADM1/TSLC1 expression in ATLL-derived lymphomas

We examined immunohistochemical staining of 90 tissue samples from patients with various types of lymphoma, including 36 patients with ATLL and 54 with non-ATLL lymphomas. These latter cases included T- or NK cell lymphomas, B-cell lymphomas, and null-cell lymphomas. Using a four-grade scale to score CADM1 immunohistochemical staining (0 to 3+), we observed that 92% of ATLL lymphomas were positive for CADM1/TSLC1.[33] Of these, 50% stained heavily for CADM1 and scored 2+ or higher. Specific membranous staining was typically observed in ATLL cells. Among the non-ATLL lymphomas, a small number of CADM1-positive cells (fewer than 5% ; score 1+) were observed. These cells were small to medium-sized and contained non-atypical, normochromatic round/ovoid nuclei. Based on these morphological and CADM1-staining analyses, the CADM1-positive cells in the non-ATLL lymphomas were not considered to be lymphoma cells but possibly histiocytes, including dendritic cells. This was suspected because these cells were similar to the CADM1-positive cells that were observed in reactive lymph nodes. Based on these results, a high degree of cell membrane staining for CADM1/TSLC1 with a score of 2+ may be highly specific for a diagnosis of ATLL. Furthermore, combined staining with CADM1/TSLC1 and other T-cell-specific markers may be necessary for a more accurate diagnosis of lymphoma-type ATLL.[33]

The question of why CADM1/TSLC1 is strongly expressed on the surface of various ATLL types remains unclear. We previously examined whether CADM1/TSLC1 expression is induced by HTLV-1/Tax expression, demonstrating that Tax protein expression did not activate CADM1/TSLC1 expression in JPX-9 cells. We also introduced a Tax expression vector into MOLT4 and 293T cells and determined the subsequent CADM1/TSLC1 expression levels. With these analyses, we demonstrated that Tax was not able to induce CADM1/TSLC1 expression in these cells, suggesting that Tax expression is unrelated to high CADM1/TSLC1 expression. Because HBZ is known to be constitutively expressed in both HTLV-1-infected and ATLL cells and can modulate host transcription,[22] it is possible that HBZ activates CADM1/TSLC1 expression. We also speculate that

high CADM1 expression in ATLL cells may be associated with transcriptional abnormalities in ATLL cells via the accumulation of genomic or epigenomic alterations. The positive correlation between HTLV-1 copy number and the percentage of $CD4^+CADM1^+$ cells in the peripheral blood of HTLV-1 carriers suggests that, if they also exhibit high percentages of $CD4^+CADM1^+$ cells, these individuals may have developed more extensive genetic alterations and may be at high risk for developing ATLL.

Recent studies have shown that certain markers, such as CCR4 and CD70, are unique ATLL surface markers.[36,37] Whereas the proportion of $CD4^+CCR4^+$ and $CD4^+CD70^+$ cells in the PBMCs of healthy individuals were observed to be approximately 5%,[37,38] the proportion of $CD4^+CADM1^+$ cells in this population was less than 1%; therefore, the measurement of $CADM1^+$ T cells is particularly efficient in the diagnosis of HTLV-1 infection in individuals who carry a small number of HTLV-1-infected cells. We have shown that CADM1/TSLC1 has important functions in increasing cell adhesion and in mediating cancer progression to organ invasion.[29] In addition, we succeeded in using anti-CADM1-coated magnetic beads to isolate low percentages of HTLV-1-infected cells from the PBMCs of HTLV-1 carriers with high HTLV-1 copy numbers, and ATLL cells from ATLL patients.[33] Sorted HTLV-1-infected and ATLL cells may be useful tools for transcriptional and/or genomic analyses. The results of such tests could be compared between the PBMCs of healthy volunteers and peripheral leukemia cells from ATLL patients, potentially providing important information with respect to the expression pattern and genomic abnormalities that occur at the early stages of HTLV-1 infection and/or ATLL development.

A recent study demonstrated that CADM1/TSLC1 directly associates with the PDZ domain of T-lymphoma invasion and metastasis 1 (Tiam1). This interaction induces the formation of lamellipodia by activating Rac in both HTLV-I-transformed cell lines and ATLL cell lines.[39] These results indicate that Tiam1 integrates signals from CADM1/TSLC1 to regulate the actin cytoskeleton through Rac activation, potentially leading to tissue infiltration of leukemic cells in ATLL patients. The elucidation of the different downstream cascades that are activated by CADM1/TSLC1 in epithelial cells and T-lymphocytes would provide important insights into the roles of CADM1/TSLC1 in tumorigenesis.

CONCLUSION

In this manuscript, we describe how CADM1/TSLC1 is highly expressed in the majority of ATLL cells and in a subset of peripheral blood cells from HTLV-1 carriers. These data suggest that CADM1/TSLC1 is potentially a prediagnostic indicator of ATLL development in high-risk HTLV-1 carriers. Therefore, we are currently developing a diagnostic kit to detect soluble CADM1/TSLC1 protein in the peripheral blood. Furthermore, we are attempting to apply this diagnostic kit to various types of ATLL patient samples, including HTLV-1 carriers. Moreover, CADM1/TSLC1 may be a novel molecular target for the treatment of ATLL. Dr. Kurosawa's group (Fujita Health University, Japan) has already developed several types of anti-human CADM1/TSLC1 antibodies using the phage-display technique and has observed that certain clones exhibited cytotoxic activity against ATLL cells (manuscript in preparation). Moreover, recombinant shuttle viruses are being developed that will target ATLL cells by binding to CRTAM and/or CADM1/TSLC1. Finally, small molecules that interfere with the cell adhesion characteristics of ATLL cells will be valuable for blocking their organ-invading ability. Thus, CADM1/TSLC1 is a clinically useful molecule for detecting and for targeting ATLL cells.

REFERENCES

1 Murakami Y: Involvement of a cell adhesion molecule, TSLC1/IGSF4, in human oncogenesis. Cancer Sci 96:543-552, 2005

2 Gomyo H, Arai Y, Tanigami A, Murakami Y, Hattori M, *et al.*: A 2MB sequence-ready contig map and a novel immunoglobulin superfamily gene IGSF4 in the LOH region of chromosome 11q23.2. Genomics 62:139-146, 1999

3 Takai Y, Irie K, Shimizu K, Sakisaka T, Ikeda W: Nectins and nectin-like molecules. Roles in cell adhesion, migration, and polarization. Cancer Sci 94:655-667, 2003

4 Yageta M, Kuramochi M, Masuda M, Fukami T, Fukuhara H, *et al.*: Direct association of TSLC1 and DAL-1, two distinct tumor suppressor proteins in lung cancer. Cancer Res 62:5129-5133, 2002

5 Masuda M, Yageta M, Fukuhara H, Kuramochi M, Maruyama T, *et al.*: The tumor suppressor protein TSLC1 is involved in cell-cell adhesion. J Biol Chem 277:31014-31019, 2002

6 Boles KS, Barchet W, Diacovo T, Cella M, Colonna M: The tumor suppressor TSLC1/NECL-2 triggers NK-cell and $CD8^+$ T-cell responses through the cell-surface receptor CRTAM. Blood 106:779-786, 2005

7 Murakami Y, Nobukuni T, Tamura K, Maruyama T, Sekiya T, *et al.*: Localization of tumor suppressor activity important in non-small cell lung carcinoma on chromosome 11q. Proc Natl Acad Sci USA 95:8153-8158, 1998

8 Kuramochi M, Fukuhara H, Nobukuni T, Kanbe T, Maruyama T, *et al.*: *TSLC1* is a tumor suppressor gene in human non-small cell lung cancer. Nat Genet 27:427-430, 2001

9 Murakami Y: Functional cloning of a tumor suppressor gene, *TSLC1*, in human non-small cell lung cancer. Oncogene 21:6936-6948, 2002

10 Fukami T, Fukuhara H, Kuramochi M, Maruyama T, Isogai K, *et al.*: Promoter methylation of the *TSLC1* gene in advanced lung tumors and various cancer cell lines. Int J Cancer 107:53-59, 2003

11 Fukuhara H, Kuramochi M, Fukami T, Kasahara K, Furuhata M,

et al.: Promoter methylation of the *TSLC1* and tumor suppression by its gene product in human prostate cancer. Jpn J Cancer Res 93:605-609, 2002

12 Sasaki H, Nishikata I, Shiraga T, Akamatsu E, Fukami T, *et al.*: Overexpression of a cell adhesion molecule, TSLC1, as a possible molecular marker for acute-type of adult T-cell leukemia. Blood 105:1204-1213, 2005

13 Yoshida M, Miyoshi I, Hinuma Y: Isolation and characterization of retrovirus from cell lines of human adult T-cell leukemia and its implication in the disease. Proc Natl Acad Sci USA 79:2031-2035, 1982

14 Takatsuki K: Discovery of adult T-cell leukemia. Retrovirology 2:16, 2005

15 Proietti FA, Carneiro-Proietti AB, Catalan-Soares BC, Murphy EL: Global epidemiology of HTLV-I infection and associated diseases. Oncogene 24:6058-6068, 2005

16 Arisawa K, Soda M, Endo S, Kurokawa K, Katamine S, *et al.*: Evaluation of adult T-cell leukemia/lymphoma incidence and its impact on non-Hodgkin lymphoma incidence in southwestern Japan. Int J Cancer 85:319-324, 2000

17 Yoshida M: Multiple viral strategies of HTLV-1 for dysregulation of cell growth control. Annu Rev Immunol 19:475-496, 2001

18 Takeda S, Maeda M, Morikawa S, Taniguchi Y, Yasunaga J, *et al.*: Genetic and epigenetic inactivation of *tax* gene in adult T-cell leukemia cells. Int J Cancer 109:559-567, 2004

19 Miyazaki M, Yasunaga J, Taniguchi Y, Tamiya S, Nakahata T, *et al.*: Preferential selection of human T-cell leukemia virus type 1 provirus lacking the 5' long terminal repeat during oncogenesis. J Virol 81:5714-5723, 2007

20 Koiwa T, Hamano-Usami A, Ishida T, Okayama A, Yamaguchi K, *et al.*: 5'-long terminal repeat-selective CpG methylation of latent human T-cell leukemia virus type 1 provirus *in vitro* and *in vivo*. J Virol 76:9389-9397, 2002

21 Taniguchi Y, Nosaka K, Yasunaga J, Maeda M, Mueller N, *et al.*: Silencing of human T-cell leukemia virus type I gene transcription by epigenetic mechanisms. Retrovirology 2:64, 2005

22 Satou Y, Yasunaga J, Yoshida M, Matsuoka M: HTLV-I basic leucine zipper factor gene mRNA supports proliferation of adult T cell leukemia cells. Proc Natl Acad Sci USA 103:720-725, 2006

23 Okamoto T, Ohno Y, Tsugane S, Watanabe S, Shimoyama M, *et al.*: Multi-step carcinogenesis model for adult T-cell leukemia. Jpn J Cancer Res 80:191-195, 1989

24 Kamada N, Sakurai M, Miyamoto K, Sanada I, Sadamori N, *et al.*: Chromosome abnormalities in adult T-cell leukemia/lymphoma : a karyotype review committee report. Cancer Res 52:1481-1493, 1992

25 Hidaka T, Nakahata S, Hatakeyama K, Hamasaki M, Yamashita K, *et al.*: Down-regulation of TCF8 is involved in the leukemogenesis of adult T-cell leukemia/lymphoma. Blood 112:383-393, 2008

26 Look AT: Oncogenic transcription factors in the human acute leukemias. Science 278:1059-1064, 1997

27 Nosaka K, Maeda M, Tamiya S, Sakai T, Mitsuya H, *et al.*: Increasing methylation of the *CDKN2A* gene is associated with the progression of adult T-cell leukemia. Cancer Res 60:1043-1048, 2000

28 Timens W: Cell adhesion molecule expression and homing of hematologic malignancies. Crit Rev Oncol Hematol 19:111-129, 1995

29 Dewan MZ, Takamatsu N, Hidaka T, Hatakeyama K, Nakahata S, *et al.*: Critical role for TSLC1 expression in the growth and organ infiltration of adult T-cell leukemia cells *in vivo*. J Virol 82:11958-11963, 2008

30 Yasuda N, Lai PK, Ip SH, Kung PC, Hinuma Y, *et al.*: Soluble interleukin 2 receptors in sera of Japanese patients with adult T cell leukemia mark activity of disease. Blood 71:1021-1026, 1988

31 Kamihira S, Atogami S, Sohda H, Momita S, Yamada Y, *et al.*: Significance of soluble interleukin-2 receptor levels for evaluation of the progression of adult T-cell leukemia. Cancer 73:2753-2758, 1994

32 Kurosawa G, Akahori Y, Morita M, Sumitomo M, Sato N, *et al.*: Comprehensive screening for antigens overexpressed on carcinomas via isolation of human mAbs that may be therapeutic. Proc Natl Acad Sci U S A 105:7287-7292, 2008

33 Nakahata S, Saito Y, Marutsuka K, Hidaka T, Maeda K, *et al.*: Clinical significance of CADM1/TSLC1/IgSF4 expression in adult T-cell leukemia/lymphoma. Leukemia [Published online : January 6, 2012, DOI: 10.1038/leu.2011.379]

34 Karube K, Ohshima K, Tsuchiya T, Yamaguchi T, Kawano R, *et al.*: Expression of FoxP3, a key molecule in $CD4^+CD25^+$ regulatory T cells, in adult T-cell leukaemia/lymphoma cells. Br J Haematol 126:81-84, 2004

35 Koma Y, Ito A, Wakayama T, Watabe K, Okada M, *et al.*: Cloning of a soluble isoform of the SglGSF adhesion molecule that binds the extracellular domain of the membrane-bound isoform. Oncogene 23:5687-5692, 2004

36 Yoshie O, Fujisawa R, Nakayama T, Harasawa H, Tago H, *et al.*: Frequent expression of CCR4 in adult T-cell leukemia and human T-cell leukemia virus type 1-transformed T cells. Blood 99:1505-15011, 2002

37 Baba M, Okamoto M, Hamasaki T, Horai S, Wang X, *et al.*: Highly enhanced expression of CD70 on human T-lymphotropic virus type 1-carrying T-cell lines and adult T-cell leukemia cells. J Virol 82:3843-3852, 2008

38 Baatar D, Olkhanud P, Sumitomo K, Taub D, Gress R, *et al.*: Human peripheral blood T regulatory cells (Tregs), functionally primed $CCR4^+$ Tregs and unprimed $CCR4^-$ Tregs, regulate effector T cells using FasL. J Immunol 178:4891-4900, 2007

39 Masuda M, Maruyama T, Ohta T, Ito A, Hayashi T, *et al.*: CADM1 interacts with Tiam1 and promotes invasive phenotype of human T-cell leukemia virus type I-transformed cells and adult T-cell leukemia cells. J Biol Chem 285:15511-15522, 2010

Leukemia (2013), 1–13

www.nature.com/leu

ORIGINAL ARTICLE

Maintenance of the hematopoietic stem cell pool in bone marrow niches by EVI1-regulated GPR56

Y Saito[1], K Kaneda[1], A Suekane[1], E Ichihara[1], S Nakahata[1], N Yamakawa[1], K Nagai[1], N Mizuno[2], K Kogawa[3], I Miura[4], H Itoh[2] and K Morishita[1]

Acute myeloid leukemia with high ecotropic viral integration site-1 expression (EVI1^{high} AML) is classified as a refractory type of leukemia with a poor prognosis. To provide new insights into the prevention and treatment of this disease, we identified the high expression of EVI1-regulated G protein-coupled receptor 56 (GPR56), and the association of high cell adhesion and antiapoptotic activities in EVI1^{high} AML cells. Knockdown of GPR56 expression decreased the cellular adhesion ability through inactivation of RhoA signaling, resulting in a reduction of cellular growth rates and enhanced apoptosis. Moreover, in *Gpr56*$^{-/-}$ mice, the number of hematopoietic stem cells (HSCs) was significantly decreased in the bone marrow (BM) and, conversely, was increased in the spleen, liver and peripheral blood. The number of *Gpr56*$^{-/-}$ HSC progenitors in the G0/G1-phase was significantly reduced and was associated with impaired cellular adhesion. Finally, the loss of GPR56 function resulted in a reduction of the *in vivo* repopulating ability of the HSCs. In conclusion, GPR56 may represent an important GPCR for the maintenance of HSCs by acting as a co-ordinator of interactions with the BM osteosteal niche; furthermore, this receptor has the potential to become a novel molecular target in EVI1^{high} leukemia.

Leukemia advance online publication, 5 April 2013; doi:10.1038/leu.2013.75

Keywords: acute myeloid leukemia; EVI1; GPR56; hematopoietic stem cell; RhoA

INTRODUCTION

Acute myeloid leukemia (AML) is a cancer of the myeloid line of blood cells, and refractory AML is considered a stem cell disease. Leukemia stem cells (LSCs) are thought to be the hijack maintenance mechanisms of hematopoietic stem cells (HSCs) in the bone marrow (BM), and consequently to contribute to eventual disease relapse after they have survived undetected in the BM niche during chemotherapy.[1,2] Therefore, if the adhesion molecules specific for LSC maintenance in the BM niche can be found, targeting these interaction molecules between LSC and the surrounding support cells could represent a promising and novel therapeutic strategy for AML.

The ecotropic viral integration site-1 (EVI1) transcription factor is a well-known marker of poor prognosis for chemotherapy-resistant AML.[3–8] The gene expression profiles found in acute myeloid leukemia with high ecotropic viral integration site-1 expression (EVI1^{high} AML) patients are quite similar to those of BM CD34^{+} cells;[9,10] EVI1 is implicated in stem cell regulation and oncogenesis, and contributes to the poor clinical outcome of AML by promoting stemness.[11] EVI1 maintains the self-renewal capacity of embryonic HSCs by activating Gata2 transcription,[12] and the ablation of EVI1 in adult BM leads to a significant decrease in the numbers of HSCs.[13] Therefore, EVI1 may have an important role in the maintenance of cell quiescence and stem cell-like phenotypes in leukemia cells, thereby contributing to their chemoresistance.

To identify novel therapeutic molecules targeting EVI1^{high} AML cells, we analyzed the gene expression profiles of these molecules and the newly identified G protein-coupled receptor 56 (GPR56) as a candidate target molecule for EVI1^{high} AML cells, along with CD52, integrin α6 and Angiopoietin-1.[14–16] GPR56 is a member of the secretin family and has been linked to developmental malformations of the human brain, known as bilateral frontoparietal polymicrogyria.[17–19] GPR56, coupled with $G\alpha_{12/13}$, induces Rho-dependent activation of transcription, resulting in actin fiber reorganization and inhibition of neural progenitor cell migration.[20] In cancer cells, overexpression of GPR56 can suppress tumor growth and metastasis in melanoma cell lines, and GPR56 functions in tumor cell adhesion in glioma cells.[21–23] Although the function of GPR56 in HSCs is still unknown,[24] GPR56 was also identified in a family of LSC-related genes correlated with a worse prognosis of AML.[11] GPR56 regulates RhoA signaling involved in cellular adhesion, and the small GTPases Rac and Cdc42 control HSC adhesion, migration and mobilization in BM niches;[25–30] therefore, we speculated that GPR56 has an important role in the maintenance of HSCs and/or LSCs in the BM niche.

In this study, we found that GPR56 was specifically expressed in EVI1^{high} AML cells as an EVI1-targeted gene and was associated with high cell adhesion and antiapoptotic activities in the leukemia cells. To further define the role of GPR56 in HSC regulation, we analyzed the function of HSCs in *Gpr56*$^{-/-}$ mice, and our results demonstrated a role of Gpr56 in maintaining HSC quiescence and osteosteal niche interactions in the BM. Because the expression of GPR56 in LSCs is higher than in HSCs, GPR56 has potential as a novel therapeutic target for EVI1^{high} AML.

[1]Division of Tumor and Cellular Biochemistry, Department of Medical Science, Faculty of Medicine, University of Miyazaki, Miyazaki, Japan; [2]Laboratory of Molecular Signal Transduction, Graduate School of Biological Sciences, Nara Institute of Science and Technology, Nara, Japan; [3]Department of Pediatrics, National Defense Medical College, Tokorozawa, Japan and [4]Division of Hematology and Oncology, Department of Internal Medicine, St Marianna University School of Medicine, Kawasaki, Japan. Correspondence: Dr K Morishita, Division of Tumor and Cellular Biochemistry, Department of Medical Science, Faculty of Medicine, University of Miyazaki, 5200 Kihara, Kiyotake, Miyazaki 889-1692, Japan.
E-mail: kmorishi@med.miyazaki-u.ac.jp
Received 15 October 2012; revised 4 March 2013; accepted 6 March 2013; accepted article preview online 12 March 2013

MATERIALS AND METHODS

Cell lines

UCSD/AML1 and HNT34 cells were cultured in RPMI1640 (Roswell Park Memorial Institute medium) supplemented with 10% fetal calf serum and 1 ng/ml of human granulocyte-macrophage (GM) colony-stimulating factor. U937 and K562 cells were cultured in RPMI1640 supplemented with 10% fetal calf serum, and 293T cells were cultured in Dulbecco's modified eagle medium supplemented with 10% fetal calf serum. Detailed information concerning our cell lines is available as described previously.[14]

Patient samples

Leukemia cells were obtained from AML patients before chemotherapy. A summary of the AML patient samples used in this study is presented in Supplementary Table 1. One sample with high expression of EVI1, consisting of PT9 cells, was cultured in RPMI1640 supplemented with 10% fetal calf serum and 1 ng/ml granulocyte-macrophage colony-stimulating factor.[14] This study was approved by the Institutional Review Board of the Faculty of Medicine of the University of Miyazaki. Informed consent was obtained from all donors in accordance with the Declaration of Helsinki.

Quantitative real-time reverse-transcription PCR

After extraction of total RNA using the TRIzol reagent (Invitrogen, Carlsbad, CA, USA), 1 μg of total RNA was reverse transcribed to produce complementary DNA using Reverse Transcriptase XL (AMV, avian myeloblastosis virus) (Takara-Bio Inc., Tokyo, Japan). The resulting first-strand complementary DNA was used as a template for real-time PCR. Real-time PCR was performed using MESA GREEN qPCR MasterMix Plus for SYBR assay (EUROGENTEC, Seraing, Belgium). The primers used in these experiments are listed in Supplementary Table 2. The mRNA expression levels of several genes were detected using an ABI Prism 7000 (Applied Biosystems, Foster City, CA, USA), and the data obtained were analyzed with Sequence Detection System software (Applied Biosystems) and normalized to β-actin.

Mice

Gpr56$^{-/-}$ mice were kindly provided by Genentech (South San Francisco, CA, USA).[18,19,31] C57BL/6 CD45.1 congenic mice (B6-CD45.1) were purchased from Sankyo-Lab Service (Tsukuba, Japan). For analysis of blood counts, peripheral blood (PB) from the tail vein was collected in a heparinized microtube and analyzed on a hematology analyzer (CellTac, NIHON KOHDEN, Tokyo, Japan).

Isolation of murine HSCs and flow cytometry

BM was collected from femurs and tibiae. Lin$^+$ cells were removed by immunomagnetic selection using AutoMACS magnetic-activated cell separation (Auto MACS, Miltenyi Biotec, Bergisch, Gladbach, Germany). Lin$^-$ cells were enriched for cells expressing c-Kit using Miltenyi CD117 microbeads and an AutoMACS magnetic selection device. The HSCs and myeloid progenitors were sorted by first staining Lin$^-$ BM cells with Alexa Fluor 647-conjugated anti-CD34 (RAM34; BD Bioscience, Franklin Lakes, NJ, USA), PerCP-Cy5.5-conjugated anti-CD16/32 (93; eBioscience, San Diego, CA, USA), PE-Cy5-conjugated anti-Flk2 (A2F10; eBioscience) and biotinylated anti-mGpr56 antibodies, followed by streptavidin-Allophycocyanin (APC)/Cy7 (BioLegend, San Diego, CA, USA). A rabbit anti-mGpr56 antibody was used as described previously.[20] Cells were then sorted using a JSAN cell sorter (Bay bioscience, Kobe, Japan).

RESULTS

High expression of GPR56 in EVI1^{high} AML cells

To search for novel molecular targets for EVI1^{high} AML, we recently analyzed the gene expression profiles of 12 human myeloid cell lines using an oligonucleotide microarray; from this analysis, GPR56 was identified.[14,15] In the present study, we focused on the analysis of GPR56, an orphan G protein-coupled receptor. Initially, we used quantitative real-time PCR to measure the expression of *EVI1* and *GPR56* in a panel of leukemia cell lines and primary leukemia samples (Figures 1a and b). Our results revealed that *GPR56* mRNA was significantly more highly expressed in the EVI1^{high} leukemia cell lines and patient samples than in their EVI1^{low} counterparts ($P<0.05$), and the expression of *GPR56* was highly correlated with the expression of *EVI1* (Figures 1a and b). Furthermore, based on gene expression profiles from a large number of patients with AML ($n=460$) (accession number GSE6891),[10] *GPR56* was highly expressed in EVI1^{high} AML cells compared with EVI1^{low} AML cells (Supplementary Figure 1a). In addition, the *GPR56* mRNA level associated with intermediate- and high-risk AML samples was significantly higher than that in the low-risk AML samples (Supplementary Figure 1b), suggesting that *GPR56* expression is a marker of poor prognosis in AML patients.

The expression of GPR56 was regulated by the EVI1 transcription factor

To determine whether the expression of *GPR56* is regulated by EVI1, we introduced an expression vector for EVI1-specific (shEVI1) or non-specific small hairpin RNA (shCNTL) into EVI1^{high} UCSD/AML1 and PT9 cells to establish UCSD/AML1 and PT9 cells exhibiting EVI1^{low} expression (UCSD/AML1/shEVI1, PT9/shEVI1) and control cells (UCSD/AML1/shCNTL, PT9/shCNTL). The expression of *GPR56* was significantly reduced in the UCSD/AML1/shEVI1 and PT9/shEVI1 cells compared with *GPR56* expression in parental and control cells (Figures 1c–e and Supplementary Figure 2). By contrast, the introduction of an EVI1 expression vector into U937 cells expressing EVI1^{low} produced U937 cells showing EVI1^{high} expression (U937/EVI1). The expression of *GPR56* was significantly increased in U937/EVI1 cells compared with control parental and U937/Mock cells (Figures 1f–h). To determine whether EVI1 regulates GPR56 expression, we next isolated a 3-kb fragment from the genomic promoter region of *GPR56* and inserted it in front of the firefly luciferase gene (pGL4-3.0). We created promoter DNA deletion mutants by deleting the region up to −1.5 (pGL4-1.5) or −2.4 (pGL4-2.4) kb, and the promoter activity was determined via luciferase assays after transfection into COS7 cells (Figure 2a). We found that the region between −2.4 and −3.0 kb markedly enhanced the promoter activity of *GPR56* in the presence of transfected EVI1. In addition, a possible binding sequence for the second DNA-binding domain of EVI1, GAAGAT, was found in the region between −2.4 and −3.0 kb. This binding sequence was replaced with the nucleotide sequence CCCGAC in the pGL4-3.0 plasmid (pGL4-3.0 m), and the resultant mutant plasmid completely abolished *GPR56* transcriptional activity. To confirm the DNA-binding activity of EVI1, several EVI1 deletion mutants were transfected into COS7 cells, and their *GPR56* transcriptional activity was measured (Figure 2b). The transcriptional activity of the mutant containing a deletion of the repression domain (ΔRD) showed less than half of the wild-type activity, and deletion of the second DNA-binding domain along with the eighth through the tenth zinc finger repeats (ΔD2 (8–10)) completely abolished *GPR56* transcriptional activity. In addition, the ΔD2 (8–10) EVI1 mutant protein was not precipitated by the DNA fragment of the GPR56 promoter region in chromatin immunoprecipitation assays (Figure 2c). Finally, the endogenous EVI1 protein was precipitated from UCSD/AML1 cells using the same GPR56 promoter region with the EVI1-binding site via chromatin immunoprecipitation with an anti-EVI1 antibody (Figure 2d). Therefore, EVI1 binds directly to the promoter region of *GPR56* and regulates *GPR56* expression in EVI1^{high} leukemia cells.

GPR56 regulated cell adhesion and migration in EVI1^{high} AML cells

Because high expression of GPR56 promotes tumorigenesis by enhancing the cellular adhesion of glioma cells,[21] we next compared the cell migration and adhesion abilities of leukemia

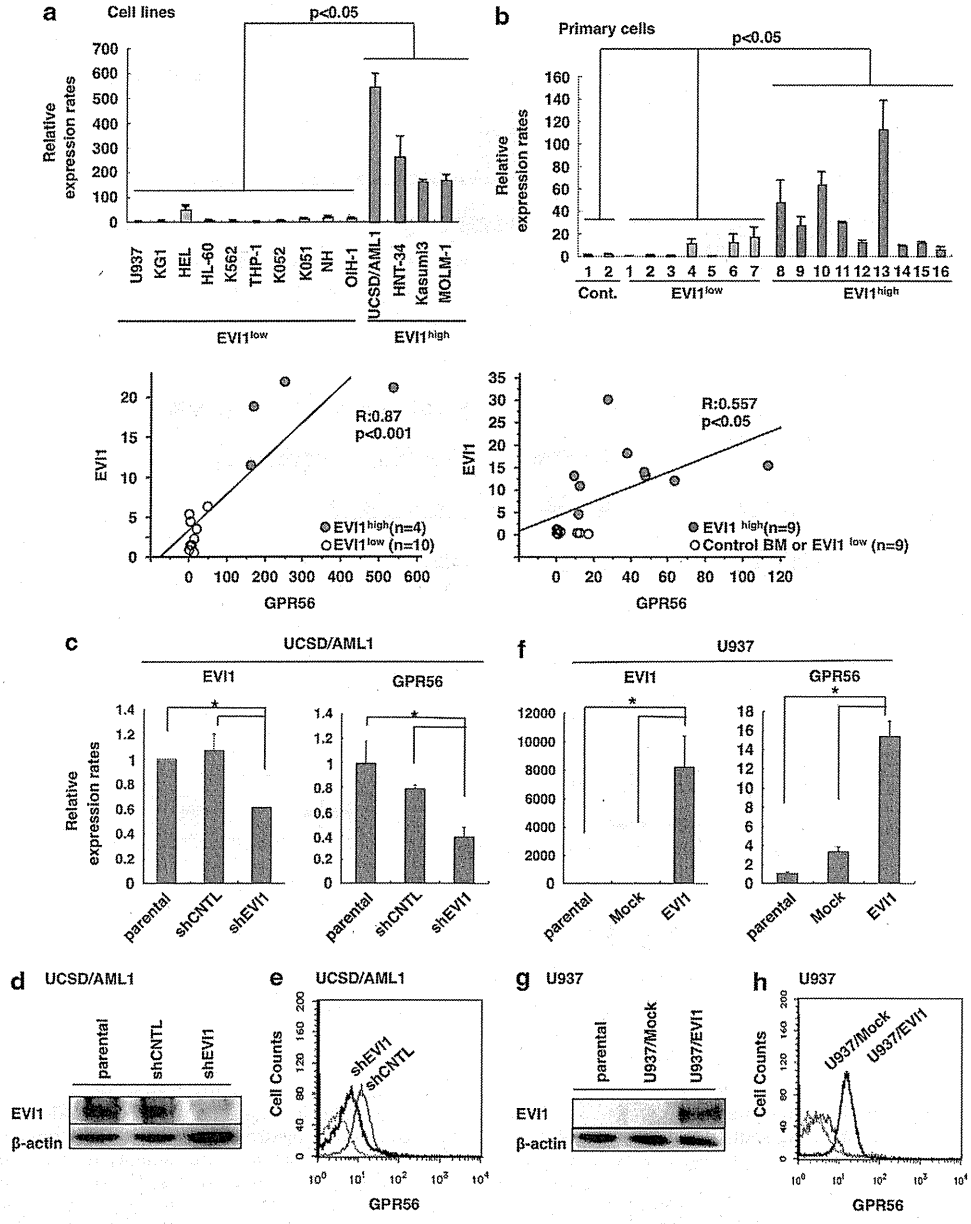

Figure 1. GPR56 is highly expressed in EVI1^{high} leukemia cells. (**a**) *GPR56* was detected in 14 AML cell lines, including 10 EVI1^{low} and 4 EVI1^{high} AML cell lines, using quantitative real-time PCR. The data are shown as the fold change in *GPR56* mRNA expression (normalized to β-actin) relative to *GPR56* expression in U937 cells. The data are presented as the means ± s.d.. The lower figure shows the correlation between the expression of EVI1 and GPR56 in the EVI1^{high} and EVI1^{low} AML cell lines based on quantitative real-time PCR analysis. The significance of the differences among the groups was assessed via a two-tailed Student's *t*-test. (**b**) *GPR56* was detected in 16 primary AML cell samples, including seven EVI1^{low} and nine EVI1^{high} AML samples. Two BM samples from healthy volunteers were used as controls. The data are shown as the fold changes in *GPR56* mRNA expression (normalized to β-actin) relative to the *GPR56* expression in control BM cells (no. 1). The data are presented as the means ± s.d. The lower figure shows the correlation between the expression of EVI1 and GPR56 in EVI1^{high} and EVI1^{low} primary AML cells and control BM samples based on quantitative real-time PCR analysis. The significance of the differences among the groups was assessed via a two-tailed Student's *t*-test. (**c**) Introduction of the small hairpin RNA (shRNA) expression vector specific for EVI1 into UCSD/AML1 cells with EVI1^{high} expression decreased GPR56 expression. Quantitative real-time reverse-transcription PCR (RT-PCR) analysis of EVI1 and GPR56 was performed in parental cells, shCNTL cells, and shEVI1 cells. The data were normalized to β-actin and are presented as relative fold changes compared with the expression in parental UCSD/AML1 cells. The data are presented as the means ± s.d. (**d**) The expression of EVI1 was downregulated in the UCSD/AML1/shEVI1 cells. EVI1 protein expression in parental UCSD/AML1, UCSD/AML1/shCNTL and UCSD/AML1/shEVI1 cells was detected using an anti-EVI1 antibody. (**e**) The cell surface expression of GPR56 in UCSD/AML1/shCNTL and UCSD/AML1/shEVI1 cells was detected by flow cytometric analysis. (**f**) The induction of GPR56 expression by forced expression of EVI1 in U937 cells expressing EVI1^{low} is shown. Quantitative real-time RT-PCR analysis of EVI1 and GPR56 was performed in parental U937 cells, U937/Mock cells and U937/EVI1 cells. The data were normalized to β-actin and are presented as relative fold changes compared with the expression in parental U937 cells. The data are presented as the means ± s.d. (**g**) EVI1 protein expression in parental U937 cells, U937/Mock cells and U937/EVI1 cells was detected with an anti-EVI1 antibody. (**h**) The cell surface expression of GPR56 in U937/Mock cells and U937/EVI1 cells was detected by flow cytometric analysis.

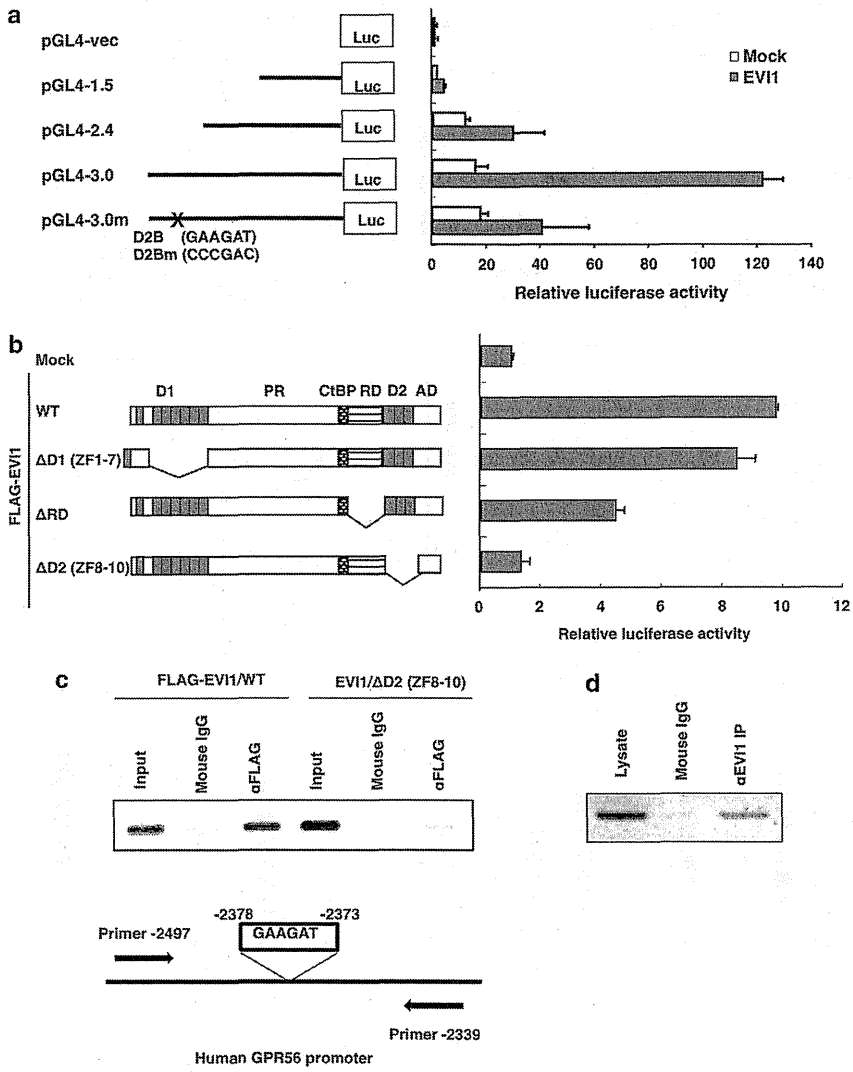

Figure 2. EVI1 binds to the promoter region of GPR56 to enhance its expression. (**a**) Structures of the GPR56 promoter region reporter plasmids are shown. A 1.5, 2.4 or 4.0 kb fragment of the GPR56 promoter region or a 4.0 kb fragment, in which GAAGAT was replaced with CCCGAC in the second ZF domain-binding sequence between −4.0 to −2.4 kb, was inserted upstream of the luciferase gene in the reporter plasmid pGL4. A mock reporter plasmid (pGL4-Vec) was used as a control. The fold change in promoter activity is shown as the ratio of normalized luciferase activity to the activity following control pGL4-Vec transfection. The open columns display the promoter activities of the various reporter plasmids, and the closed columns display the activities of a reporter plasmid in the presence of an EVI1 expression vector. All luciferase reporter assays were performed in duplicate in two independent experiments. The values and error bars depict the means ± s.d. (**b**) The structures of wild-type EVI1 and the EVI1 mutants with a series of deleted domains are depicted. COS7 cells were co-transfected with the GPR56 reporter vector, and each expression vector was co-transfected with EVI1 or EVI1 mutants (ΔD1 (ZF1-7), ΔRD, or ΔD2 (ZF8-10)). The fold change was calculated by dividing the fold activation of each EVI1 mutant co-transfected with pGL4-3.0 by the fold activation of the respective EVI1 mutant co-transfected with pGL4-vec. All of the luciferase reporter assays were performed in duplicate in two independent experiments. The values and error bars depict the means ± s.d. (**c**) Chromatin immunoprecipitation analysis of the EVI1-binding site in the GPR56 promoter region after transfection with the EVI1 expression vector is shown. After co-transfection with FLAG-tagged EVI1/WT or EVI1/ΔD2 (ZF8-10) with pGL4-3.0, formalin-fixed DNA fragments were immunoprecipitated with an anti-FLAG antibody or control mouse immunoglobulin G. The precipitated DNA was then amplified using specific primers to detect the EVI1-binding sites. (**d**) Chromatin immunoprecipitation of the endogenous EVI1 protein from UCSD/AML1 cells is shown. Formalin-fixed DNA fragments were immunoprecipitated with an anti-EVI1 antibody or control mouse immunoglobulin G. The precipitated DNA was then amplified using specific primers to detect the EVI1-binding sites.

cells with high or low GPR56 expression. After introduction of GPR56-specific small hairpin RNA or control small hairpin RNA into UCSD/AML1 cells, the expression of GPR56 was significantly decreased in UCSD/AML1/shGPR56 cells compared with the UCSD/AML1/shCNTL cell line (Figures 3a and b). The cellular adhesion of these lines was evaluated using either a feeder layer consisting of a murine osteoblastic cell line, MC3T3-E1, or using plates coated with fibronectin, Matrigel, laminin-1 or collagen type III. The adhesion of UCSD/AML1/shGPR56 cells to MC3T3-E1 cells and the various types of extracellular matrix was significantly impaired compared with that of the parental and UCSD/AML1/shCNTL cells (Figure 3c). Similar results were obtained for PT9 cells

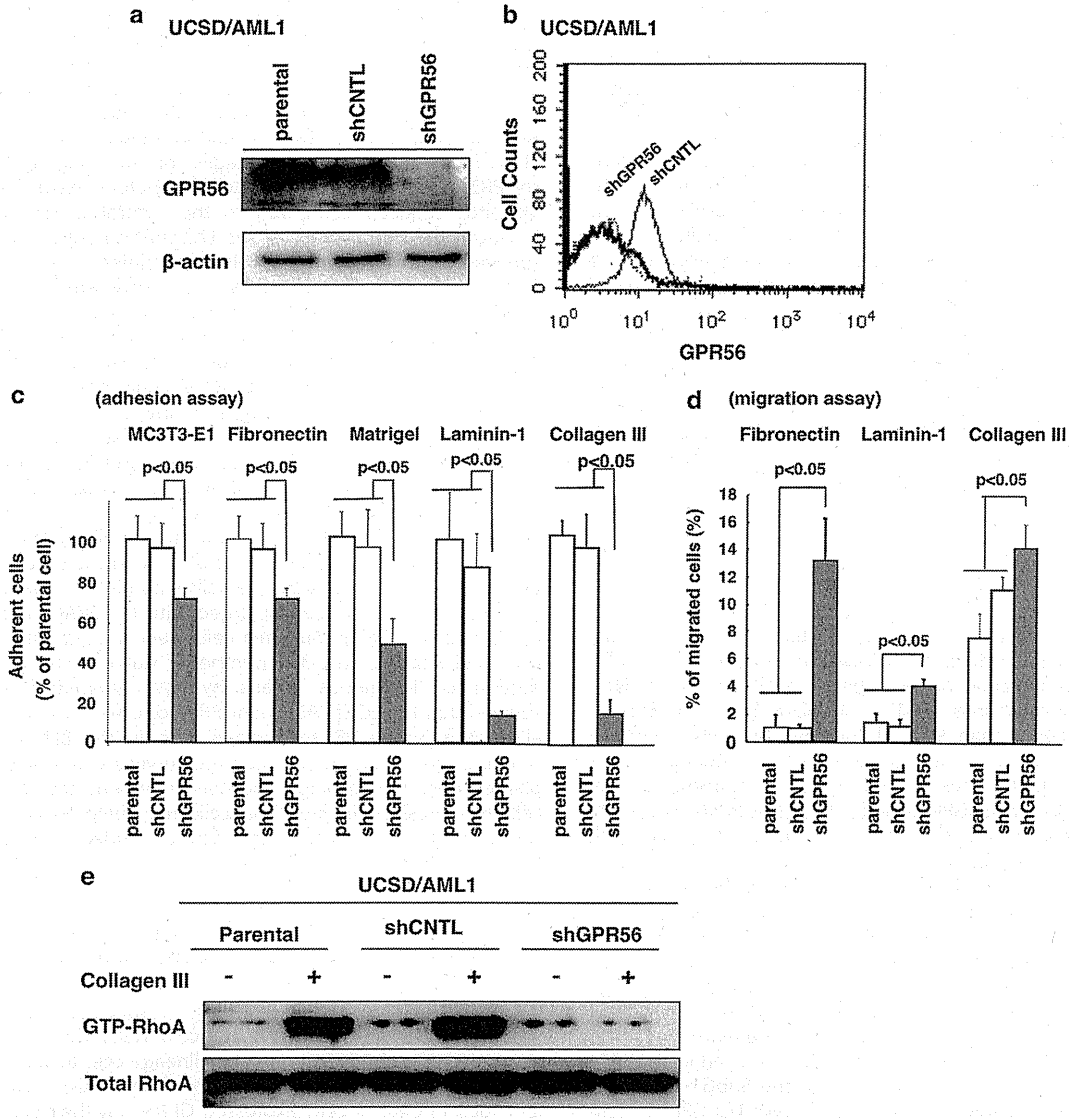

Figure 3. Knockdown of GPR56 expression increases the cell migration ability and decreases cellular adhesion to the extracellular matrix (ECM) through activation of the RhoA pathway. (**a**) Introduction of the shGPR56 expression vector into UCSD/AML1 cells downregulated GPR56 protein expression. The expression of GPR56 in parental UCSD/AML1, UCSD/AML1/shCNTL and UCSD/AML1/shGPR56 cells was detected with an anti-GPR56 antibody. (**b**) The cell surface expression of GPR56 in UCSD/AML1/shCNTL and UCSD/AML1/shGPR56 cells was determined by flow cytometric analysis. (**c**) The adhesion of parental UCSD/AML1, UCSD/AML1/shCNTL and UCSD/AML1/shGPR56 cells to MC3T3-E1 or ECM (fibronectin, Matrigel, laminin-1 or collagen type III) was quantified. The data are presented as the means ± s.d of the relative fold changes compared with the adherent cells in parental UCSD/AML1 cells. (**d**) The migration activities of the parental UCSD/AML1, UCSD/AML1/shCNTL and UCSD/AML1/shGPR56 cells through an ECM layer of fibronectin, laminin-1 or collagen type III were measured in response to an stromal cell-derived factor-1 (SDF-1α) gradient. The percentages of migrated cells are shown compared with the total cell numbers in this experiment. The data are presented as the means ± s.d. (**e**) The activated form of RhoA in parental UCSD/AML1, UCSD/AML1/shCNTL and UCSD/AML1/shGPR56 cells was measured via western blot analysis. The level of total RhoA in the cell lysates served as an internal control.

transfected with shGPR56 (PT9/shGPR56) (Supplementary Figures 3a and b). By contrast, the adhesion of U937/GPR56 cells was significantly increased compared with that of the parental and U937/Mock cells (Supplementary Figures 3c and d). To determine the cell migration abilities of the leukemia cells, the cells were added to the upper well of a Boyden chamber after fibronectin, laminin-1 or collagen type III had been embedded at the interface, and culture medium containing stromal cell-derived factor-1 was added to the bottom chamber. The number of migrating UCSD/AML1/shGPR56 cells was significantly increased compared with that of the parental and UCSD/AML1/shCNTL cells in the three different types of coated chambers (Figure 3d). Because the expression of CXCR4 was not significantly different between both cell types (Supplementary Figure 4), the increased migration ability mainly depended on the adhesion ability of the cells to the extracellular matrix in a Boyden chamber.

Collagen type III and other extracellular matrix molecules induce activation of the small GTP-binding protein RhoA downstream of GPR56;[31] therefore, we next determined the protein levels of GTP-bound RhoA in these cell lines. The level of GTP-bound RhoA in

parental and UCSD/AML1/shCNTL cells was increased after stimulation by collagen type III. However, the GTP-bound RhoA content in nonstimulated AML/shGPR56 cells was lower than the content in control cell lines, and stimulation with collagen type III did not increase the amount of GTP-bound RhoA in AML/shGPR56 cells (Figure 3e). To confirm whether activation of RhoA is necessary for the cellular adhesion of AML cells showing high GPR56 expression, Y-27632, a selective inhibitor of the Rho-associated protein kinase p160ROCK, was added to the culture medium of UCSD/AML1 cells. In control medium, UCSD/AML1 cells attached to conventional culture plates with a spindle-shaped cell morphology. However, the morphology of UCSD/AML1 cells changed from dendritic to small and round after the treatment with Y-27632 (Supplementary Figure 5a). In addition, the adhesion of UCSD/AML1 cells to MC3T3-E1 cells or to fibronectin was significantly decreased by treatment with Y-27632 (Supplementary Figure 5b). Therefore, the high level of cellular adhesion of EVI1^{high} AML cells was partially dependent on the expression of GPR56, and downstream RhoA activation has an important role in regulating cellular adhesion and cell migration in EVI1^{high} AML cells.

Involvement of GPR56 expression in apoptosis of EVI1^{high} AML cells

In the next set of experiments, we determined whether the expression of GPR56 affects the growth and viability of EVI1^{high} AML cells. After infection of recombinant shGPR56- or shCNTL-containing lentivirus into EVI1^{high} UCSD/AML1 and EVI1^{high} HNT34 cells, greater than 90% of the infected cells were GFP positive. Cell growth was determined immediately after infection. The growth rates of both cell lines transduced with shGPR56 (UCSD/AML1/shGPR56 and HNT34/shGPR56) were significantly decreased 3–5 days after infection compared with the growth rates of parental and shCNTL-infected cells (Figures 4a and b). Moreover, after introduction of the shGPR56 expression vector into PT9 cells, the colony-forming ability of parental PT9, PT9/shCNTL and PT9/shGPR56 cells was determined in methylcellulose cultures with GM- colony-stimulating factor. The colony number and size of granulocyte/macrophage colony-forming units were significantly reduced in PT9/shGPR56 cells (Supplementary Figures 6a and b). Therefore, we next determined whether apoptotic cell death was induced in shGPR56 cells. In a cell cycle analysis, an increase in the SubG1-phase cell population was observed in the UCSD/AML1/shGPR56 cells (Figure 4c). To confirm the induction of apoptotic cell death by GPR56 knockdown, lentivirus-infected cells were analyzed via flow cytometry after double staining with 7-Aminoactinomycin D and phycoerythrin-conjugated Annexin V (Figures 4d and e). The population of apoptotic cell death in the UCSD/AML1/shGPR56 cells was significantly increased compared with that in the UCSD/AML1/shCNTL cells several days after lentiviral infection, suggesting that the apoptosis of the UCSD/AML1/shGPR56 cells was due to the reduction of GPR56 expression. To determine the molecular mechanism underlying the inhibition of the apoptosis pathway downstream of GPR56 signaling, we determined the protein expression status of known apoptotic indicators and cell cycle regulators, including p53 and caspase-3 (Figure 4f). Cleaved caspase-3 fragments were detected in UCSD/AML1/shGPR56 cells, indicating that the apoptotic pathway was activated. Interestingly, the protein levels of p53, p21 and p27 were increased in UCSD/AML1/shGPR56 cells, whereas the level of MDM2 was proportionally decreased. However, the mRNA levels of p53 and MDM2 were unchanged in UCSD/AML1/shGPR56 cells compared with control UCSD/AML1 cells (Supplementary Figure 7), suggesting that an unknown signaling pathway downstream of GPR56 may stabilize the level of the MDM2 protein in EVI1^{high} AML cells, which promotes cell survival by promoting p53 degradation.

GPR56 expression was related to cell adhesion mediated drug resistance and the invasion ability of leukemic cells in BM

We next examined the role of GPR56 expression in the drug sensitivity of the cells to anticancer drugs. The UCSD/AML1 cells were seeded on MC3T3-E1 or BSA with various concentrations of Ara-C or daunorubicin (DNR) in culture media. Twenty-four hours after incubation, the percentages of surviving UCSD/AML1/shGPR56 cells on MC3T3-E1 cells (adherent status) were significantly reduced compared to the control UCSD/AML1 cells; however, the percentages of the UCSD/AML1/shGPR56 cells that survived under conventional culture condition were not different between the cells (Figures 5a and b). To determine the role of GPR56 expression in drug resistance *in vivo*, we performed xenotransplantation experiments of leukemia cells with high or low GPR56 expression into non-obese diabetic-severe combined immunodeficiency/γcnull (NOD-SCID/γcnull, NOG) mice. Initially, we determined the percentages of invaded leukemia cells in various organs two weeks after transplantation. Leukemia cells with high GPR56 expression (K562/GPR56 and UCSD/AML1) had a tendency to infiltrate into the BM more than other organs; however, leukemia cells with low GPR56 expression (K562/Mock and UCSD/AML1/shGPR56) infiltrated to the PB and other organs more than the BM (Figures 5c and d). To find the different effects of anticancer drugs on leukemia cells with high or low expression of GPR56 *in vivo*, mice transplanted with UCSD/AML1/shCNTL or UCSD/AML1/shGPR56 leukemia cells were treated with Ara-C for two weeks; at this time, the number of viable leukemia cells was determined in various organs by flow cytometry. The result showed that the USCD/AML1/shGPR56 cells were more effectively eliminated in the PB and spleen than in the BM (Figure 5e). Although we did not determine the survival curve of xenotransplanted mice undergoing anticancer treatment, the reduction of GPR56 expression in leukemia cells may help to enhance the sensitivity to anticancer drugs; further studies are needed to examine these effects.

High GPR56 expression in murine hematopoietic stem cell fractions and decreased numbers of HSCs in the BM of *Gpr56*$^{-/-}$ mice

Because GPR56, regulated by EVI1, is speculated to have an important function in the maintenance of HSCs, we next examined the expression of GPR56 in myeloid lineage cells at various stages of differentiation via flow cytometry analysis. Over 90% of LSK (Lin$^-$Sca-1$^+$c-Kit$^+$) cells expressed GPR56 on their cell surfaces, and more primitive self-renewing HSCs, including long-term and short-term HSCs, showed expression rates greater than 95% (Supplementary Table 3 and Supplementary Figure 8a). The level of GPR56 expression gradually decreased during the myeloid differentiation stages, and less than 50% of Lin$^+$ progenitor cells exhibited detectable GPR56 expression. In the BM in the diaphysis of tubular bones, high numbers of GPR56-positive cells were detected by fluorescence staining close to the periosteal rim, which is a region that contains potential BM osteosteal niches. The GPR56-positive mononuclear cells frequently coexpressed c-Kit and Sca-1, suggesting that GPR56$^+$c-Kit$^+$ primitive cells may localize near the periosteal region (Figure 6a and Supplementary Figure 8b). To determine the role of GPR56 in the regulation of hematopoiesis, we initially confirmed the downregulation of GPR56 expression in Lin$^-$ BM cells in *Gpr56*$^{-/-}$ mice (Supplementary Figure 9a), and determined the hematological profiles in their PB. There were no differences in the blood cell counts or hemoglobin content between the wild-type and *Gpr56*$^{-/-}$ mice (Supplementary Table 4). There were also no differences in whole-BM cells and spleen cells (Supplementary Figure 9b). Interestingly, the percentages of LSK cells in the BM were significantly decreased, but the percentages in the spleen and the PB were conversely increased in the *Gpr56*$^{-/-}$ mice

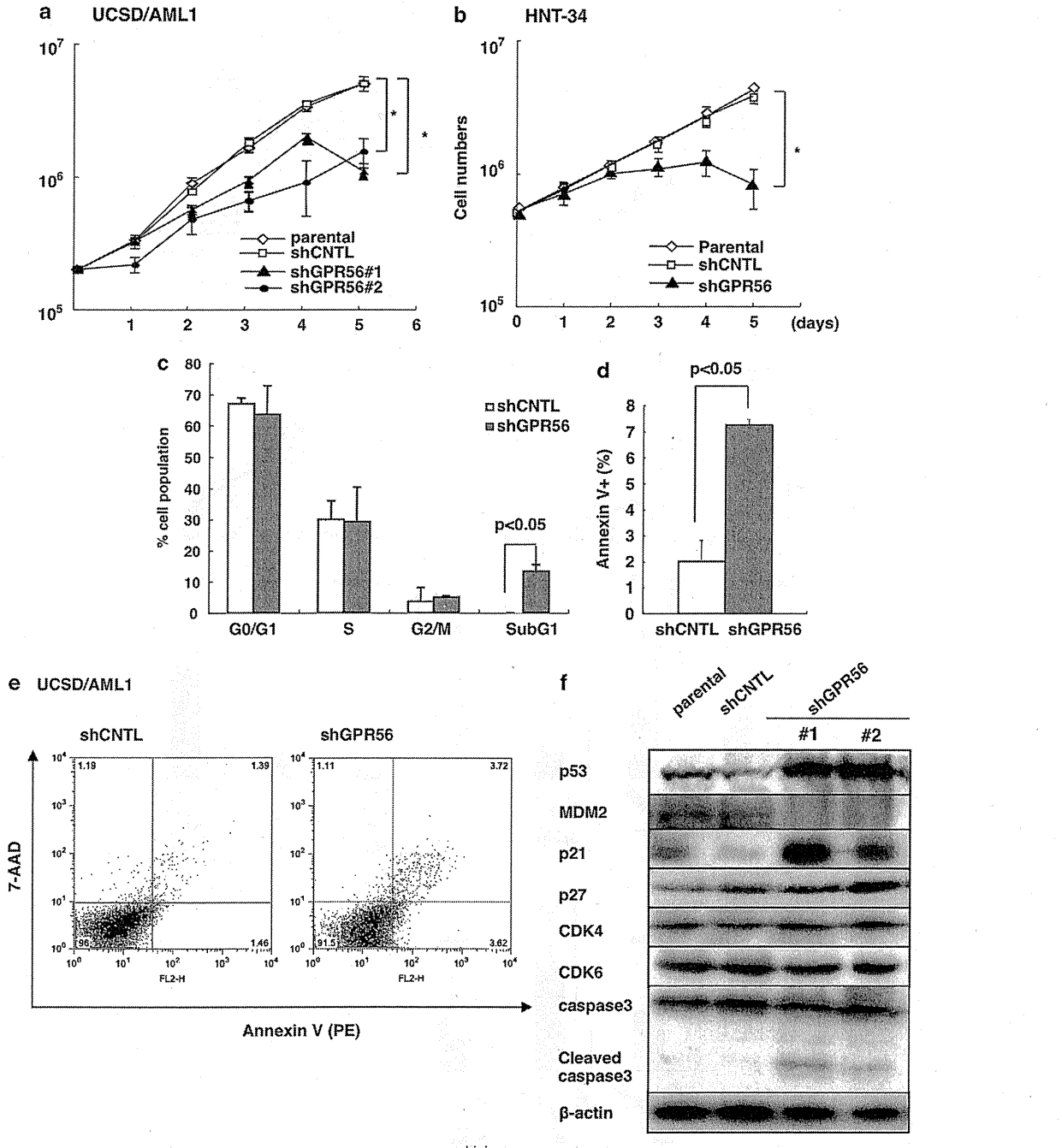

Figure 4. Knockdown of GPR56 expression induced apoptosis in EVI1^{high} leukemia cells through the accumulation of p53. (**a** and **b**) The influence of GPR56 knockdown on cell proliferation is shown. The growth rates of parental UCSD/AML1, UCSD/AML1/shCNTL and UCSD/AML1/shGPR56 cells and parental HNT34, HNT34/shCNTL and HNT34/shGPR56 cells were evaluated with the trypan blue exclusion assay. The live cells were counted after trypan blue staining using light microscopy. The data are presented as the means ± s.d. (**c**) Cell cycle fractions were analyzed by fluorescence-activated cell sorting after propidium iodide staining. The data are presented as the means ± s.d. (**d** and **e**). Six days after cell culture, UCSD/AML1/shCNTL and UCSD/AML1/shGPR56 cells were labeled with Annexin V and 7-aminoactinomycin D (7-AAD) and analyzed by flow cytometry. The percentages of Annexin V-stained dead cells are displayed as a bar graph (**d**), and the biparametric histogram represents the apoptotic cells, which show high Annexin V and low 7-AAD signals, and the secondary necrotic cells, which show high Annexin V and high 7-AAD signals (**e**). The experiments were performed in triplicate and repeated independently at least three times. (**f**) The expression of a series of apoptosis-related proteins was analyzed in various types of UCSD/AML1 cells by western blotting. Knockdown of GPR56 induced the accumulation of p53 by reducing the level of MDM2.

(Figures 6b and c). Moreover, the populations of short-term HSCs and long-term-HSCs were significantly reduced among the BM cells of the *Gpr56*$^{-/-}$ mice (Figure 6d). In the next experiment, we determined the colony-forming ability of mononuclear cells from the BM, spleen, liver and PB using semi-solid culture with several specific cytokines (Figure 6e). The number of granulocyte/

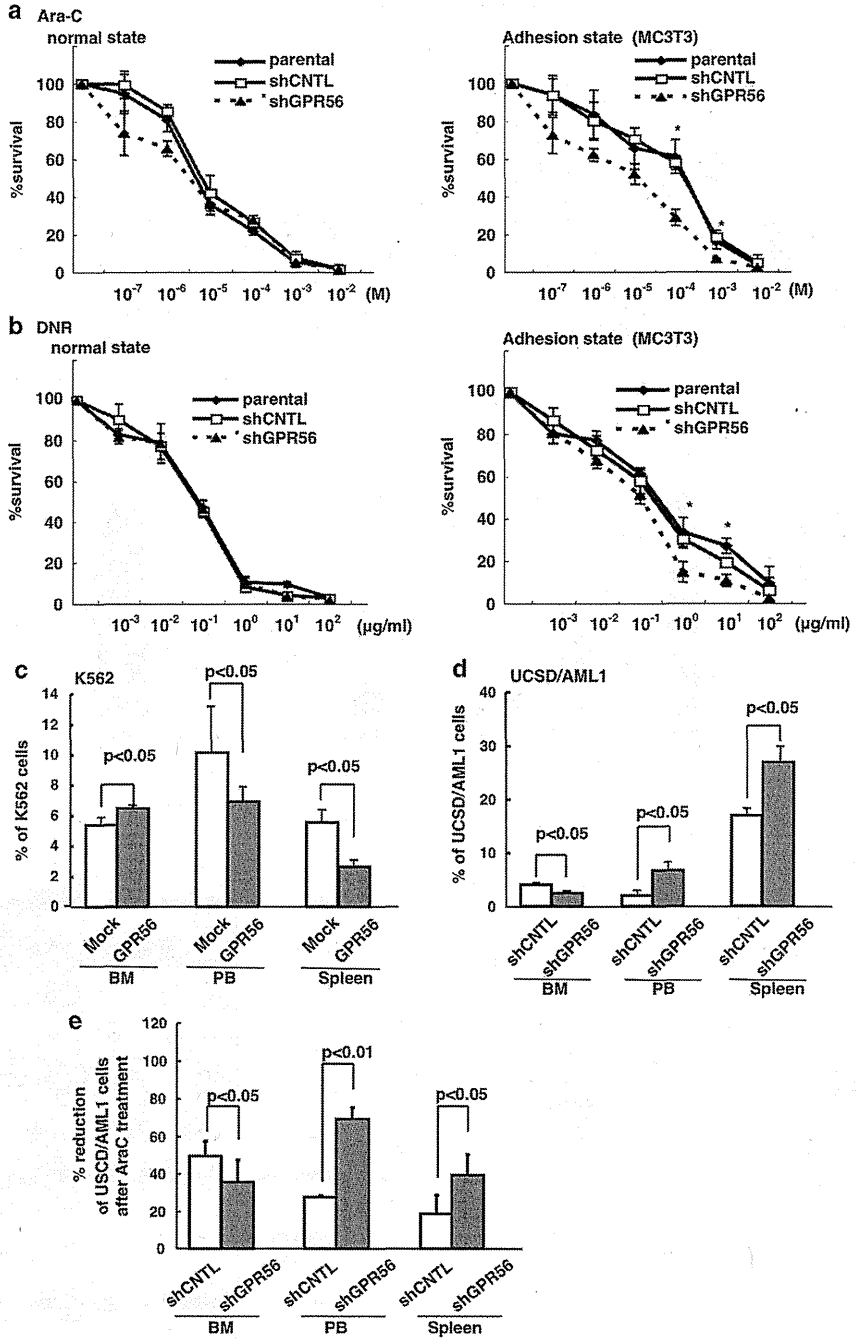

Figure 5. Knockdown of GPR56 inhibits drug resistance in AML cells, and GPR56 is an important regulator of leukemic cell engraftment. (**a** and **b**) The effect of adhesion on the chemosensitivity of UCSD/AML1, UCSD/AML1/shCNTL and UCSD/AML/shGPR56 cells is shown. UCSD/AML1 cells were incubated with Ara-C (**a**) or DNR (**b**) on MC3T3 coated plates. The number of viable cells and percentage of viable cells were assessed by trypan blue exclusion. The data are presented as the means ± s.d. Asterisks denote $P < 0.05$ by Student's *t*-test. (**c**) K562/Mock cells or K562/GPR56 cells were intravenously transplanted into non-obese diabetic-severe combined immunodeficiency/γcnull (NOD-SCID/γcnull, NOG) mice. Two weeks after transplantation, the mice were killed, and the percentage of migration was analyzed. The means ± s.e. ($N = 5$ per group), as evaluated by Student's *t*-test, are shown. (**d**) UCSD/AML1/shCNTL cells or UCSD/AML1/shGPR56 cells were intravenously transplanted into NOG mice. Two weeks after transplantation, the mice were killed, and the percentage of migration was analyzed. The means ± s.e. ($N = 5$ per group), as evaluated by Student's *t*-test, are shown. (**e**) Mice were treated with Ara-C intravenously once per week (150 mg/kg). Two weeks after being treated with Ara-C, the mice were killed, and the percentage of the reduction in the leukemia cells was analyzed.

macrophage colony-forming units was significantly decreased in the BM of *Gpr56*$^{-/-}$ mice. However, granulocyte/macrophage colony-forming units and granulocyte, erythrocyte, monocyte/macrophage, megakaryocyte colony-forming unit (CFU-GEMM) numbers were clearly increased in the spleen, liver and PB of *Gpr56*$^{-/-}$ mice. Because the total colony numbers of